Geobios 93 (2025) 99–115

Contents lists available at ScienceDirect

Geobios

journal homepage: www.elsevier.com/locate/geobio

Research Paper

Early Miocene fossils from Shaoma, China, evidence Eurasia-North America ruminant exchange ☆

Shi-Qi Wang [a,*], Tao Deng [a,b], Tingjiang Peng [c], Bian Wang [a,b], Qigao Jiangzuo [a,b], Jiao Fu [a,b], Danhui Sun [a,b], Luda Xing [a,b]

[a] Key Laboratory of Vertebrate Evolution and Human Origins of Chinese Academy of Sciences, Institute of Vertebrate Paleontology and Paleoanthropology, Chinese Academy of Sciences, Beijing 100044, China
[b] University of Chinese Academy of Sciences, Beijing 100049, China
[c] Lanzhou University, Lanzhou 730000, China

ARTICLE INFO

Article history:
Received 22 January 2025
Accepted 6 June 2025
Available online 11 June 2025

Keywords:
Pecoran
New genus and species
Phylogeny
Xiejian
Hezuo Basin
Tibetan Plateau

ABSTRACT

Stem pecorans radiated globally near the Oligocene–Miocene boundary but remain poorly documented in China. We report a new stem pecorans, *Labrangomeryx dorcapolis* nov. gen., nov. sp. and previously reported *Sinopalaeoceros xiejiaensis*, from the earliest Miocene (~23–20 Ma) of Gansu, China. *Labrangomeryx* nov. gen. exhibits bunoselenodont dentition with unique traits: a bifurcated p4 anterior conid, strong metastylids, and absent entoconulid in molars, linking Eurasian and North American taxa (e.g., *Pomelomeryx*, *Problastomeryx*). *Sinopalaeoceros* displays high hypsodonty and m3 entoconulid, resembling North American merycodontines rather than later Asian bovids. Both taxa lack cranial appendages, pointing towards a placement within stem pecorans. An enigmatic large p4 may present a tylopodan affinity, implying North American ties. These findings reveal early pecoran diversification in Eastern Asia and underscore transcontinental faunal exchanges during the early Miocene, bridging Eurasian and North American evolutionary narratives. The absence of crown-family cranial features highlights unresolved systematic positions but enriches understanding of pecoran morphological plasticity during their initial radiation.

1. Introduction

The Xiejian Stage, the initial Neogene stage in China, corresponds to the MN 1–3 of the Early Miocene (Meng et al., 2013; Qiu et al., 2013). Defined by the Xiejia Fauna from the Xining Basin along the Tibetan Plateau's northwestern margin (Li and Qiu, 1980), this stage represents a transitional evolutionary phase between Oligocene and Miocene mammalian assemblages. Xiejian fossil mammals predominantly consist of small Late Oligocene relicts exhibiting derived features but lacking distinctive taxa (Li and Qiu, 1980; Qiu et al., 2013), resulting in relatively few confirmed Xiejian Age localities. These include the Xiejia, Zhangjiaping, Gaolanshan, and Lower Aoerban faunas, along with the Suosuoquan II–III biozones (Qiu et al., 2013)..

Although Central Asia is regarded as an evolutionary center for stem and crown pecoran ruminants (Vislobokova, 1997), Xiejian records provide limited insights into ruminant evolution. The sole documented species, *Sinopalaeoceros xiejiaensis* (originally described as *Oioceros*? *xiejiaensis*; Chen, 1988), shows questionable bovid affinities due to the absence of horn cores – a critical diagnostic feature of Bovidae. Other indeterminate specimens are tentatively classified as Cervidae or Bovidae, but no definitive horn cores or antlers have been recovered from these deposits so far.

The Hezuo Basin (Fig. 1) is a small intermountainous fault basin located in the western part of a low-relief, high-elevation plateau surface (Meiwu Plateau surface; Ma et al., 2021; Fig. 1), on the northeastern margin of the Tibetan Plateau. Cenozoic deposits of this basin are ca. 150 m thick and primarily consist of reddish siltstone and mudstones in the upper layers, with sandstones and conglomerates at the bottom (Ma et al., 2021). The basin is rich in fossil mammals. The preliminary identification reveals that the fossil assemblage includes *Amphechinus kansuensis*, *Litodonomys lajeensis*, *Plesiosminthus*? sp., *Sicista* sp., *Heterosminthus firmus*, *Heosminthus borrae*, *Eucricetodon* sp., *Plesiosciurus* sp., *Proansomys*

☆ Corresponding editor: Laurent Marivaux.
* Corresponding author.
E-mail address: wangshiqi@ivpp.ac.cn (S.-Q. Wang).

https://doi.org/10.1016/j.geobios.2025.06.002

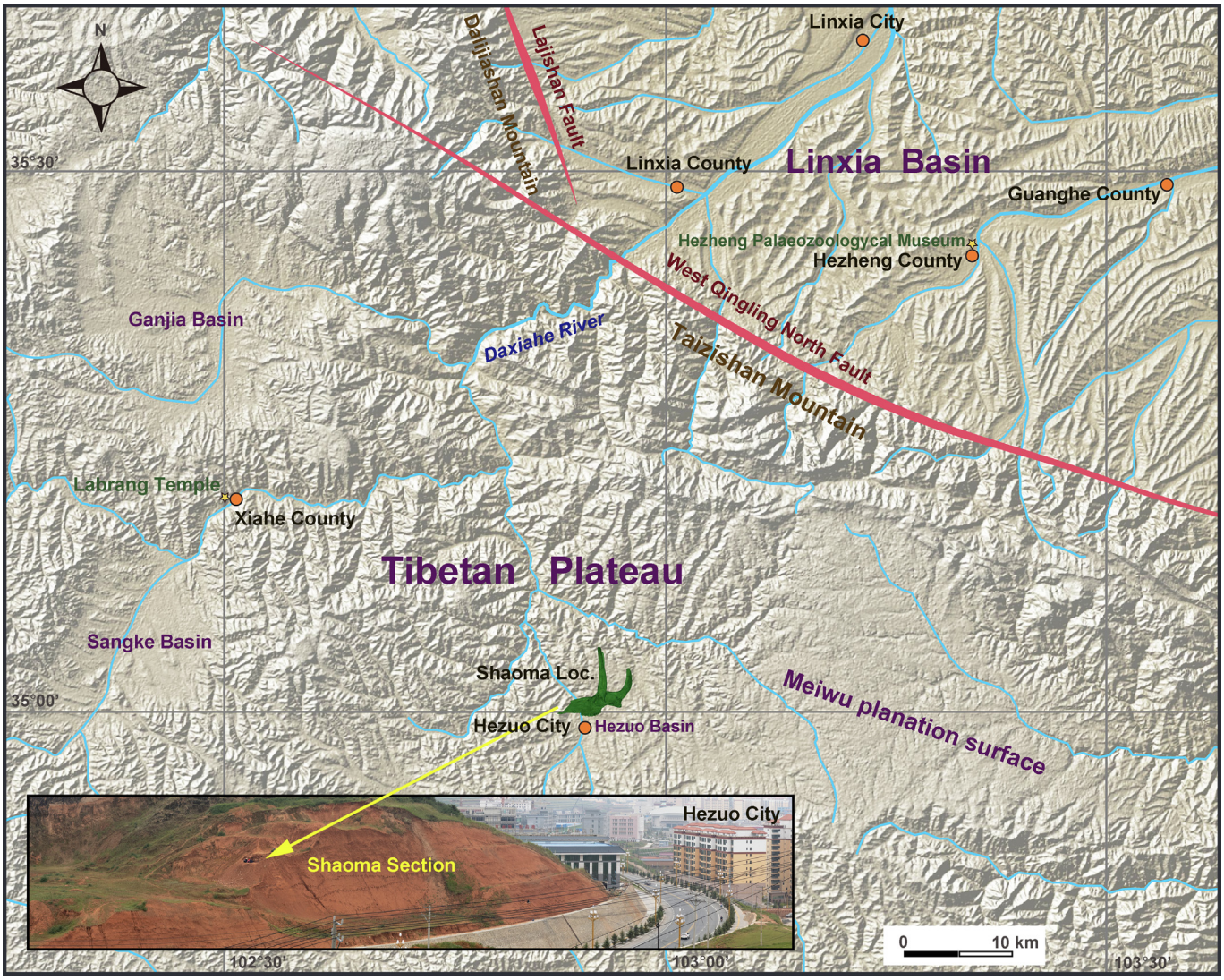

Fig. 1. Topological map showing the location of the Shaoma fossil locality (Gansu, China), along with some geological and geomorphological features of the adjacent area. The insert panel shows a photo of the fossil quarry.

dureensis, Aplodontidae? gen. et sp. indet., *Alldistylomys* sp., *Yindirtemys deflexus*, *Tachyoryctoides* sp., *Sinolagomys* sp., *Desmatolagus* sp., *Aprotodon* sp., *Diaceratherium* sp., Suiform? gen. et sp. indet., Protoceratidae? gen. et sp. indet., *Labrangomeryx dorcapolis* nov. gen., nov. sp., and *Sinopalaeoceros xiejiaensis*. Key biostratigraphic markers include *Sinopalaeoceros xiejiaensis* and *Litodonomys lajeensis* (previously exclusive to the Xiejia Locality; Li and Qiu, 1980), *Heterosminthus firmus* and *Alldistylomys* (restricted to the Xiejian Lower Aoerban biozone), and shared Xiejian taxa such as *Amphechinus*, *Plesiosminthus*, *Heterosminthus*, *Sicista*, *Eucricetodon*, *Proansomys*, *Yindirtemys*, *Tachyoryctoides*, *Desmatolagus*, and *Aprotodon*. Stratigraphic links to the Late Oligocene Tabenbulukian (*A. kansuensis*, *Y. deflexus*, *H. borrae*, *P. dureensis*) and Early Miocene Shanwangian (*Diaceratherium*, *Plesiosciurus*) underscore the fauna's transitional nature, strongly supporting its correlation to the Xiejian Age.

2. Material and methods

All examined fossil materials are housed in the Institute of Vertebrate Palaeontology and Palaeoanthropology (IVPP), with comparative specimens curated at the American Museum of Natural History (AMNH), New York, USA, and Naturhistoriches Museum Basel (NMB), Basel, Switzerland. Ruminant cheek teeth terminology follows Bärmann and Rössner (2011) (Fig. 2). Measurements were obtained using a caliper with the precision of 0.01 mm.

A cladistic analysis was performed to examine the phylogenetic relationships among genera and species within ruminants. We constructed a morphological data matrix including 41 taxa and 46 characters based on Mennecart and Métais (2015) and our own scoring (Texts S1, S2; Appendix A). *Amphirhagatherium weigelti* (Choeropotamidae) and *Merycoidodon culbertsoni* (Merycoidodontidae) were selected as the outgroup (Texts S1, S2; Data S1; Appendix A). The most parsimonious reconstructions were performed using TNT v.1.1 (Goloboff et al., 2008). The result was reported as a strict consensus tree (Code S1; Appendix A).

3. Results

3.1. Systematic paleontology

Class Mammalia Linnaeus, 1758
Order Artiodactyla Owen, 1848
Suborder Ruminantia Scopoli, 1777

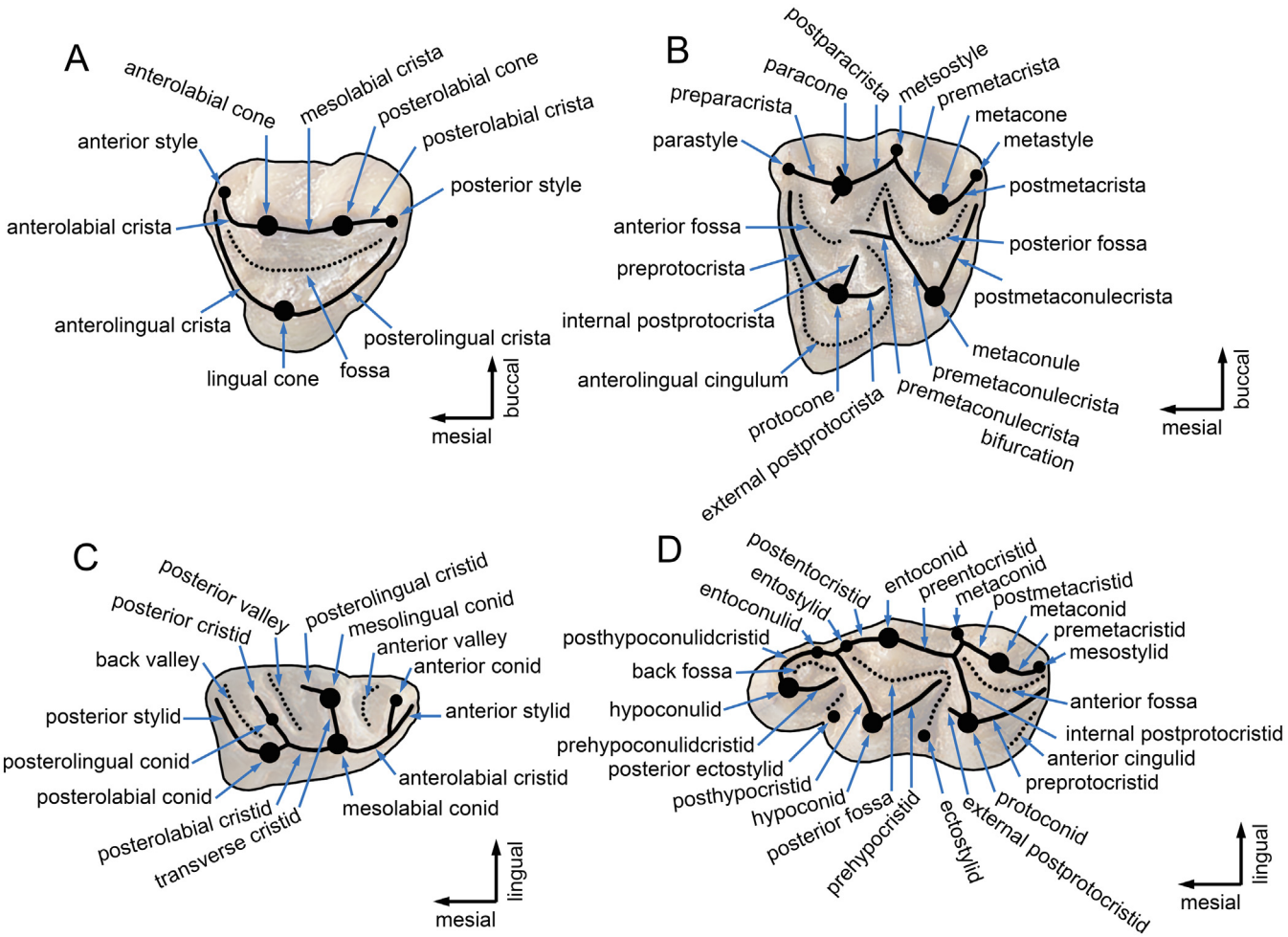

Fig. 2. Premolar and molar terminology of pecorans, slightly revised after Bärmann and Rössner (2011). **A.** Upper premolar. **B.** Upper molar. **C.** Lower premolar. **D.** Lower molar.

Family indet.

Genus ***Labrangomeryx*** nov. gen.

LSID: urn:lsid:zoobank.org:act:0FAC6047-F054-43C4-8998-1BE46F82807A

Derivation of the name: The genus name *Labrang* derives from the renowned Tibetan Buddhist monastery near the fossil locality (Fig. 1), one of the six principal Gelugpa schools of Tibetan Buddhism, reflecting its cultural significance in the region. The suffix *-meryx* originates from the Greek term for ruminant.

Type and only species: *Labrangomeryx dorcapolis* nov. gen., nov. sp.

Occurrence: Early Miocene (MN 1–3), northern China.

Diagnosis: Small pecoran with markedly bunoselenodont and brachyodont cheek teeth. P2 bearing a distinct labial cone; labial cone of P3 shifted mesially; secondary structures on upper cheek teeth (external postprotocrista, enamel spurs, and fossal folds) strongly developed; M3 displaying a pronounced anterolingual cingulum. p4 featuring a bifurcated anterior conid and a moderately developed mesolingual conid with an incipient posterolingual cristid; lower molars with unaligned metaconid and entoconid; metastylids, ectostylids, and external postprotocristids moderate to strongly expressed; postentocristid complete; m3 presenting a ring-like posterior fossa, lacking a definitive entoconulid.

Differential diagnosis: *Labrangomeryx dorcapolis* differs from all hornless pecorans in the mesial shift of the P3 labial cone; from *Dremotherium*, *Hydropotopsis*, *Bendenomeryx*, *Walangania*, *"Amphitragulus" feningrei*, and *Pomelomeryx gracilis* in more bunoselenodont and brachydont cheek teeth; from *Andegameryx*, *Friburgomeryx*, and *Babameryx* in the presence of moderate to strong metastylids, ectostylids, and external postprotocristids; from *Amphitragulus*, *Oriomeryx*, and *Pomelomeryx boulangeri* in the bifurcated p4 anterior conid, ring-like m3 posterior fossa, and absence of an entoconulid; from *Problastomeryx*, *Parablastomeryx*, and *Pseudoblastomeryx* in more brachydont teeth and stronger external postprotocristids; from Cervidae in lacking antlers, possessing more bunoselenodont-brachydont cheek teeth, and absence of an entoconulid; and from Moschidae in the combination of bunoselenodont-brachydont cheek teeth, lack of entoconulid, and p4 missing an anterolingual cristid.

Labrangomeryx dorcapolis nov. gen., nov. sp.

Fig. 3

LSID: urn:lsid:zoobank.org:act:F8E4E5E4-6BE7-4506-A71F-0D4F8E74ACC6

Derivation of the name: *dorc-*, gazelle or antelope; *-polis*, city. This name dedicates to the Hezuo City (fossil locality), which is nicknamed "Antelope City".

Holotype: IVPP V33528, fragmentary left hemimandible bearing p3–m3.

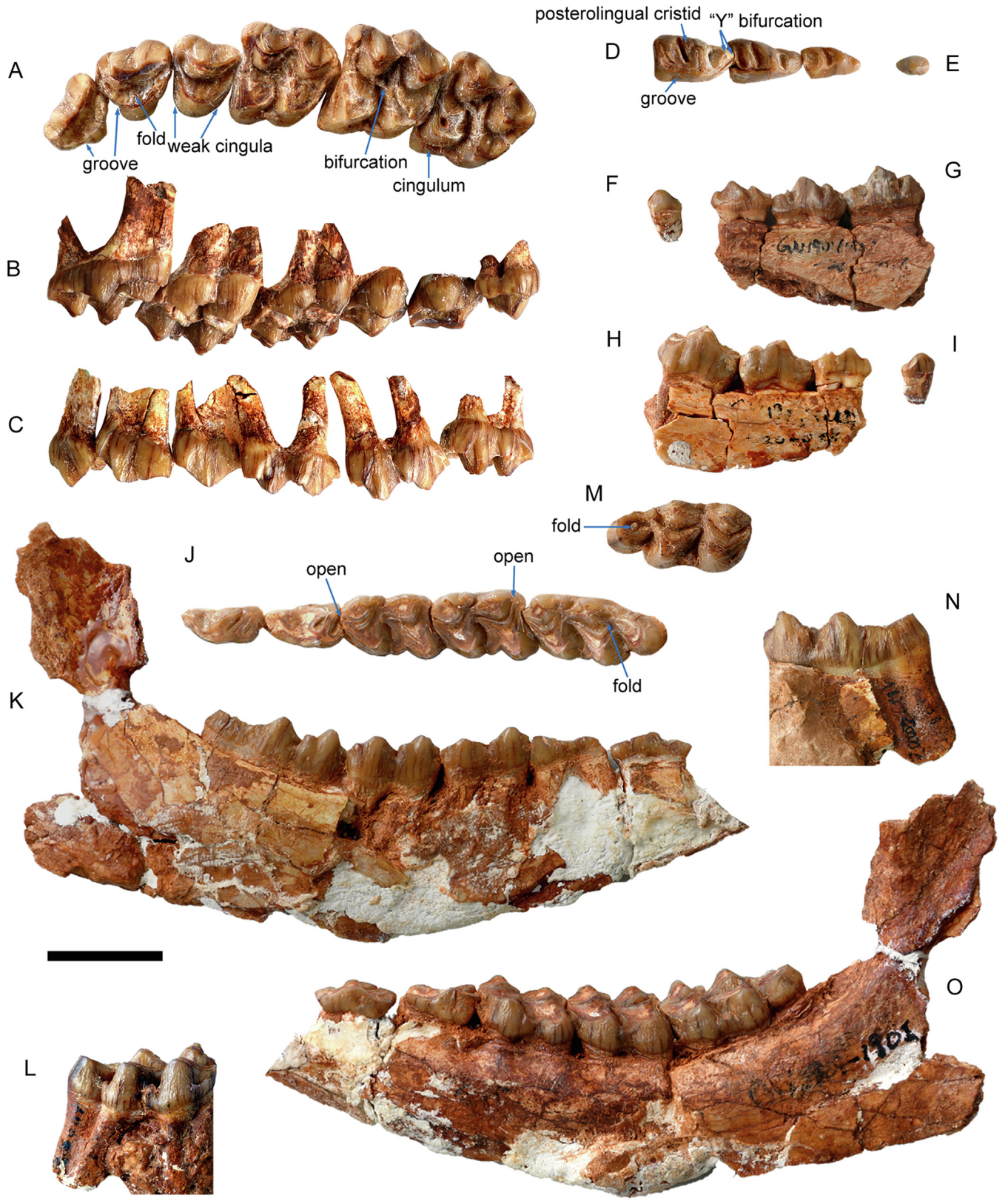

Fig. 3. *Labrangomeryx dorcapolis* nov. gen., nov. sp. from the Shaoma fossil locality (Gansu, China). **A**–**C**. IVPP V33532, left P2–M3 in occlusal, lingual, and buccal views. **E**, **F**, **I**. IVPP V33531, right p1 in occlusal, lingual, and buccal views. **D**, **G**, **H**. IVPP V33530, right hemimandible bearing p2–p4 in occlusal, lingual, and buccal views. **J**, **K**, **O**. V33528, holotype, left hemimandible bearing p3–m3 in occlusal, lingual, and buccal views. **L**–**N**. V33529, right m3 in buccal, occlusal, and lingual views. Scale bar: 10 mm.

Paratypes: IVPP V33529, right m3; V33530, fragmentary right hemimandible bearing p2–p4; V33531, right p1; V33532, left upper jaw bearing P2–M3.

Type locality and horizon: Shaoma (IVPP GN201901), Hezuo City, Gansu Province; Linxia Fm., Early Miocene, Xiejian.

Occurrence: Early Miocene (MN 1–3), northern China.

Measurements: See Table 1.

Diagnosis: As for the genus, by monotypy.

Descriptions:

Upper cheek teeth. The upper jaw (IVPP V33532) preserves P2–M3 (Fig. 3(A–C)). The P2 exhibits a triangular morphology with minimal elongation. The lingual cone is prominent and slightly displaced mesially. A robust, buccally oriented anterior style connects to the lingual cone via a curved anterolingual crista, which is linked to the lingual cone but retains a lingual groove. The anterolabial cone is pronounced, displaying a buccal apex and a slender anterolabial crista. The posterolabial cone is nearly vestigial, with a thickened posterolabial crista directly extending to a weakly developed posterior style. The posterolingual crista is nearly linear and converges with the posterolabial crista, though the fossa remains distally open due to the lack of fusion between these cristae. Two or three faint enamel folds occur along the lingual margin of the fossa. In buccal view, the anterolabial cone is elevated, characterized by a thick buccal rib merging with the anterior style rib, while the posterior style rib is absent.

The P3 morphology closely resembles that of P2 (Fig. 3(A–C)). It retains a triangular outline but is broader than P2. The lingual cone is robust, featuring a bulbous lingual profile and being strongly displaced mesially, aligning with the anterolabial cone. Alongside the pronounced anterolabial cone, the posterolabial cone is faintly inflated and joined to the anterolabial cone via a narrowed mesolabial crista. The distal end of the posterolingual crista ends immediately adjacent to the posterior style, forming a minor distal notch. A prominent central fold originates from the lingual cone apex, accompanied by smaller folds emerging at the fossal base. In buccal view, the posterolabial cone rib becomes distinct and closely parallels the robust anterolabial cone rib.

The P4 is short and wide (Fig. 3(A–C)). The lingual cone is large and bulbous. A long anterolingual crista encloses the mesial margin of the tooth, connecting to a prominent anterior style. The labial cone is robust, globular, and lingually inflated. The anterolabial crista is thinner and shorter than the posterolabial crista, extending into a moderately developed posterior style. Central folds are faint yet complex. Faint remnants of anterolingual and posterolingual cingula are present but largely indistinct. In buccal view, alongside the robust ribs of the labial cone and anterior style, a weakly defined posterior style rib emerges.

The M1–M3 exhibit highly similar morphology (Fig. 3(A–C)). The M2 is marginally larger than the M1 and M3. In occlusal view, the molars are nearly square-shaped, except for the M3, which displays a slightly reduced metaconule. The protocone of M1 and M2 is triangular under moderate wear, whereas that of M3 is quadrangular. The preprotocrista is elongated, extending to the parastyle. The external postprotocrista is distinct, distally oriented, and diverges from the internal postprotocrista at a wide angle. Both internal and external postprotocristae are abbreviated, resulting in a distally open anterior fossa. The paracone is globular, inflated buccally and lingually, generating pre- and postparacristae that connect to the robust parastyle and mesostyle, respectively. The metacone is triangular and exclusively lingually inflated. In M3, the metacone is more lingually displaced, misaligned with the paracones compared to M1 and M2. The metastyle is weakly developed in M1 and M2 but markedly pronounced in M3. The metaconule is relatively large and sub-rounded in M1 and M2, slightly reduced in M3, and assumes a triangular outline. The prominent premetaconulecrista approaches yet remains separate from the lingual aspect of the mesostyle. A bifurcation of premetaconulecrista projects toward the anterior fossa, terminating at the paracone's lingual border. The posterior fossa of M1 and M2 (particularly M2) remains distally open due to incomplete postmetaconulecrista

Table 1
Measurements (in mm) of the artiodactyl cheek teeth from the Shaoma fossil locality, Gansu, China. The "+" sign indicates a tooth with more than lightly wear, making true high larger than the measurement.

Specimen nb.	taxon	locality	Locus	L	W	H
V33532	*L. dorcapolis*	Shaoma	P2	7.26	5.29	4.88
V33532		Shaoma	P3	7.58	6.79	4.78
V33532		Shaoma	P4	5.99	7.35	5.28
V33532		Shaoma	M1	9.34	10.41	4.89
V33532		Shaoma	M2	9.42	11.4	4.92
V33532		Shaoma	M3	8.99	10.8	4.99
V33531		Shaoma	p1	3.10	1.79	2.78
V33530		Shaoma	p2	5.39	2.69	3.00
V33530		Shaoma	p3	6.31	3.80	4.11
V33528		Shaoma	p3	7.11	3.42	3.2+
V33530		Shaoma	p4	7.57	4.13	4.79
V33528		Shaoma	p4	7.20	4.12	3.2+
V33528		Shaoma	m1	8.29	6.39	4+
V33528		Shaoma	m2	9.03	6.88	4.1+
V33528		Shaoma	m3	13.05	7.5	4.2+
V33529		Shaoma	m3	12.75	6.81	4.49
V33536	*S. xiejiaensis*	Shaoma	P2	5.21	4.88	4.9+
V6008		Xiejia	DP4	6.58	7.01	5.42
V6007		Xiejia	M1	6.5+	6.19	6+
V6007		Xiejia	M2	8.42	7.86	7.37
V33535		Shaoma	M2	8.59	8.61	9.61+
V6008		Xiejia	M2	7.99	6.62	8.91+
V6008		Xiejia	M2	7.61	7.09	8.62+
V33534		Shaoma	p4	6.61	3.20	5.60
V6008		Xiejia	m1	6.6+	–	–
V6008		Xiejia	m2	8.59	4.37	13.22
V33533		Shaoma	m2	7.29	5.77	7.9+
V33533		Shaoma	m3	13.38	4.38	14.79
V33554	Protoceratidae? gen. et sp. indet.	Shaoma	p4	18.10	12.42	11.20

development, whereas it is fully enclosed in M3. A metaconule fold is present. In M1 and M2, the anterolingual cingulum is moderately developed, with a minute entostyle closely appressed to the metaconule. In M3, the anterolingual cingulum encircles the lingual margin of protocone, but the entostyle is nearly absent. In lingual view, the molars are brachydont, featuring pyramidal parastyle and mesostyle ribs, alongside a thick, columnar paracone rib. M1 and M2 exhibit a faint metacone rib, absent in M3. Conversely, the M3 metastyle rib is prominent, merging directly with the mesostyle rib basally.

Mandibles and lower cheek teeth. IVPP V33528, the holotype, is a fragmentary left hemimandible bearing p3–m3 (Fig. 3(J, K, O)). The region anterior to p3 and the ramus are extensively fractured. The remaining corpus is shallow and faintly dorsally curved.

IVPP V33531 is an isolated p1 (Fig. 3(E, F, I)). The tooth is diminutive, featuring a globular mesoconid from which a short anterolabial cristid and a comparatively elongated posterolabial cristid extend.

IVPP V33530 is a partial mandible bearing p2–p4 (Fig. 3(D, G, H)). The premolars are brachydont and bunodont, characterized by brevity, moderate mediolateral inflation, and morphological uniformity. The p2 is small, displaying a conical mesolabial conid with a robust distally oblique transverse cristid, lacking a mesolingual conid. A diminutive anterior conid connects to the mesolabial conid via a short anterolabial cristid. The posterolabial conid links to the mesolabial conid through a flexed posterolabial cristid. The posterolingual conid and posterior stylid are nearly parallel and oriented buccally.

The p3 exhibits a triangular outline, possessing a mesolabial conid more elevated than that of m2 (Fig. 3(D, G, H)). The distally oblique transverse cristid is more pronounced than in m2, while the mesolingual conid remains undifferentiated. The anterior conid is larger, and the anterolabial cristid longer, compared to those of p2. A diminutive anterior stylid is present. The posterolingual conid is slightly obliquely oriented, and the posterior stylid curves distally, enclosing the tooth's distal margin. These structures originate from a weakly developed posterolabial conid, which connects to the mesolabial conid via a short posterolabial cristid.

The p4 is relatively shorter and broader than p2 and p3 (Fig. 3 (D, G, H)). The trigonid is more developed, while the talonid is comparatively reduced. The anterior stylid is distinctly separated from the anterior conid, forming a Y-shaped structure. The anterolabial cristid is elongated and curved. The mesolabial conid is elevated, displaying a short, robust, and predominantly lingually oriented transverse cristid. A blunt mesolingual conid is delineated; further, a very small posterolingual cristid is apposed to the distolingual aspect of the mesolingual conid. The posterolabial conid is weakly developed, separated from the mesolabial conid by a lingual groove. The posterolingual conid is obliquely positioned, bearing a faint posterior cristid. The posterior stylid delineates the distal margin of p4.

The lower molars are moderately brachydont and bunodont. The morphology of m1 and m2 is nearly identical, with m1 being slightly smaller than m2 (Fig. 3(J, K, O)). They are moderately broad, exhibiting a length slightly exceeding the width. The trigonid is moderately narrower than the talonid. The metaconid and entoconid are misaligned, positioned at a minor angle relative to one another. The metaconid is globular and inflated labiolingually. The mesostylid is weakly developed, whereas the metastylid is large and rounded. The protoconid displays a rounded buccal profile. The preprotocristid fails to connect to the premetacristid, resulting in an open anterior fossa. The external postprotocristid (*Palaeomeryx*-fold) is robust and abbreviated, originating from the protoconid apex. The internal postprotocristid converges with the junction of the postmetacristid and preentocristid, forming a Y-shape structure. The entoconid is similarly globular; the postentocristid is well-defined, extending to the distolingual margin of the tooth and generating a distally oriented diminutive entostylid. The hypoconid also exhibits a rounded buccal contour. The prehypocristid approaches the distal wall of the internal postprotocristid but remains discontinuous. The posthypocristid incompletely encloses the posterior fossa distally, creating a minor notch. The ectostylid is moderately developed. In the m1 and m2 of V33528 (holotype), deep wear facilitates its fusion to the prehypocristid's mesial wall. In lingual view, the metaconid and entoconid ribs are thickened and blunt. The metastylid rib is prominent, contrasting with the faint mesostylid and entostylid ribs.

The m3 comprises three lobes, with the anterior two lobes mirroring the morphology of m1 and m2 (Fig. 3(D, G, H, J, K, O)). In the isolated m3 (IVPP V33529), the metastylid is comparatively smaller (Fig. 3(J, K, O)). The hypoconulid is robust, and the entoconulid remains indistinct. The third lobe forms a ring-like structure enclosing the back fossa. The posterior ectostylid is markedly diminutive. In IVPP V33528 (holotype; Fig. 3(J, K, O)), a prominent enamel fold occurs at the posterior fossa's distal terminus. In contrast, the isolated m3 (IVPP V33529; Fig. 3(L, M)) lacks this fold but exhibits a distinct enamel fold within the back fossa.

Remarks: In *Labrangomeryx dorcapolis* nov. gen., nov. sp., the premolars are relatively short and wide, the p4 bears a moderately enlarged mesolingual conid, the external postprotocristid persists, the metacone rib is faintly developed, the metastylid is pronounced, and the cheek teeth are distinctly brachydont and bunoselenodont – features collectively diagnostic of a hornless pecoran. Notably, no cranial appendages have been identified from this locality.

During the latest Oligocene and earliest Miocene, hornless pecorans were abundant in Europe and North America, with additional records in South Asia and Africa, yet they remained scarce in Central and Eastern Asia. In Europe, these taxa have been comprehensively studied. Historically, European hornless pecorans were classified under two canonical genera: *Amphitragulus* and *Dremotherium*. Recent revisions, however, recognize greater diversity, encompassing *Pomelomeryx*, *Bendenomeryx*, *Oriomeryx*, *Andegameryx*, *Friburgomeryx*, and *Babameryx*. *Labrangomeryx dorcapolis* nov. gen., nov. sp. distinguishes itself from these genera through a key autapomorphy: the pronounced mesial displacement of the lingual cones in P2 and particularly P3 – a rare trait among early pecorans. Beyond this feature, *L. dorcapolis* nov. gen., nov. sp. shares closest affinities with the early Miocene (MN 1–3) genus *Pomelomeryx*, especially *P. boulangeri*, with overlapping size for these two species (Fig. 4(A–C)). Shared characteristics include brachydont-bunoselenodont cheek teeth, abbreviated upper premolars, an inflated P2 lingual cone, a weakly developed p4 posterolingual cristid, moderately developed ectostylid and external postmetacristid, narrow notches at the mesiolingual and distolingual margins of m1–m2, and a fully enclosed m3 back fossa. Nonetheless, *L. dorcapolis* nov. gen., nov. sp. diverges from *P. boulangeri* (excluding *P.* cf. *boulangeri* from Wintershof-West, which shares the mesially displaced P3 lingual cone; Obergfell, 1957; Rössner, 1995) in retaining a p1, exhibiting more robust secondary structures in upper molars (e.g., external postprotocrista, enamel spurs/folds within fossae), stronger metastylids, and a bifurcated p4 anterior stylid. Another congeneric species, *P. gracilis*, the type species of *Pomelomeryx* (Ginsburg, 1985), is smaller than *L. dorcapolis* nov. gen., nov. sp. (Fig. 4(A–C)). While *P. gracilis* shares a p1 and comparably developed upper molar secondary structures, it markedly differs in its heightened selenodonty (e.g., laterally compressed metaconid/entoconid, sharply defined lingual margins of protoconid/hypoconid). These morphological disparities challenge

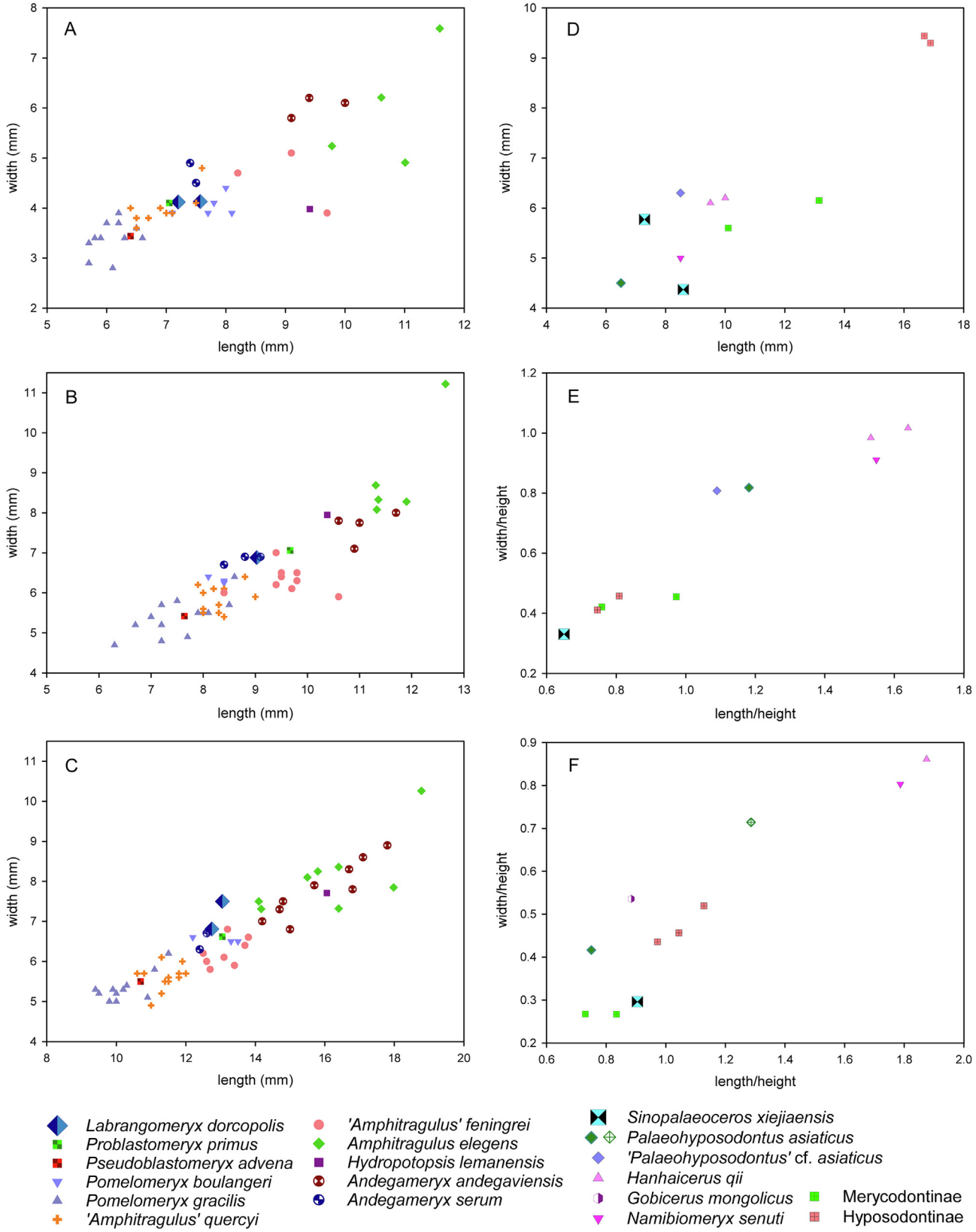

Fig. 4. Biometric comparisons of cheek teeth of *Labrangomeryx dorcapolis* nov. gen., nov. sp. (A–C) from the Shaoma fossil locality (Gansu, China) and *Sinopalaeoceros xiejiaensis* (D–F). **A–D**. length vs. width of p4 (A), m2 (B, D), and m3 (C). **E, F**. ratio of length to height vs. ratio of width to height of m2 (E) and m3 (F). Note that in F, both sample points of *Palaeohypsodontus asiaticus* are from the same specimen, PIN 473-93. The green diamond represents the original measurements in Trofimov (1958), and the open diamond with a crossing represents the revised measurement in Huang (1985). Other data sources: *Problastomeryx primus* and *Pseudoblastomeryx falkenbachi*, measured in AMNH collection; *Pomelomeryx boulangeri* (see Obergfell, 1957; Ginsburg et al., 1991; Rössner and Rummel, 2001); *P. gracilis* (see Rössner and Rummel, 2001); "*Amphitragulus*"*quercyi* and "*A.*" *feningrei* (see Mennecart, 2012); *A. elegans* (see Ginsburg et al., 2001) and measured in NMB collection; *Hydropotopsis lemanensis* measured in NMB collection; *Andegameryx andegaviensis* (see Ginsburg, 1971); *A. serum* (see Obergfell, 1957); "*Palaeohypsodontus* cf. *asiaticus*" and *Hanhaicerus qii* (see Huang, 1985), *Gobicerus mongolicus* (see Sokolov, 1952); *Namibiomeryx senuti* (see Morales et al., 1995); Merycodontinae measured in AMNH collection; Hypsodontinae measured in IVPP collection.

the generic attribution of *P. boulangeri* (Rössner and Rummel, 2001).

Amphitragulus represents a significant genus of European hornless pecorans characterized by relatively bunoselenodont dentition (contrasting with the more primitive *Dremotherium*). The Oligocene species "*A.*" *quercyi*, "*A.*" *feningrei*, and *A. primaevus* have been retained within this genus, though the first two remain taxonomically contested (Mennecart, 2015). Among Miocene taxa, only *Amphitragulus elegans* (Fig. 5(A, B)) is retained in the genus, while others – including *Pomelomeryx gracilis*, *P. boulangeri*, *Amphitragulus lemanensis*, and *Oriomeryx major* – have been reassigned to distinct genera (Ginsburg, 1985; Ginsburg and Morales, 1989; Ginsburg et al., 1991). Within the genus's stratigraphic scope (encompassing Late Oligocene species and Early Miocene *A. elegans*), "*A.*" *quercyi* – the smallest taxon (marginally smaller than *L. dorcapolis* nov. gen., nov. sp.; Fig. 4(A–C)) – has been hypothesized as the ancestral precursor to *Pomelomeryx* (Mennecart, 2012). "*Amphitragulus*" *quercyi* retains a p1 but diverges from *L. dorcapolis* nov. gen., nov. sp. in lacking a p4 anterior stylid, displaying an incomplete postentocristid, reduced metastylid, and weakly developed cingulids. "*Amphitragulus*" *feningrei*, another species tentatively assigned to the genus, is distinguished from other *Amphitragulus* species by its marginally more selenodont cheek teeth (Mennecart, 2012), a trait further differentiating it from *L.*

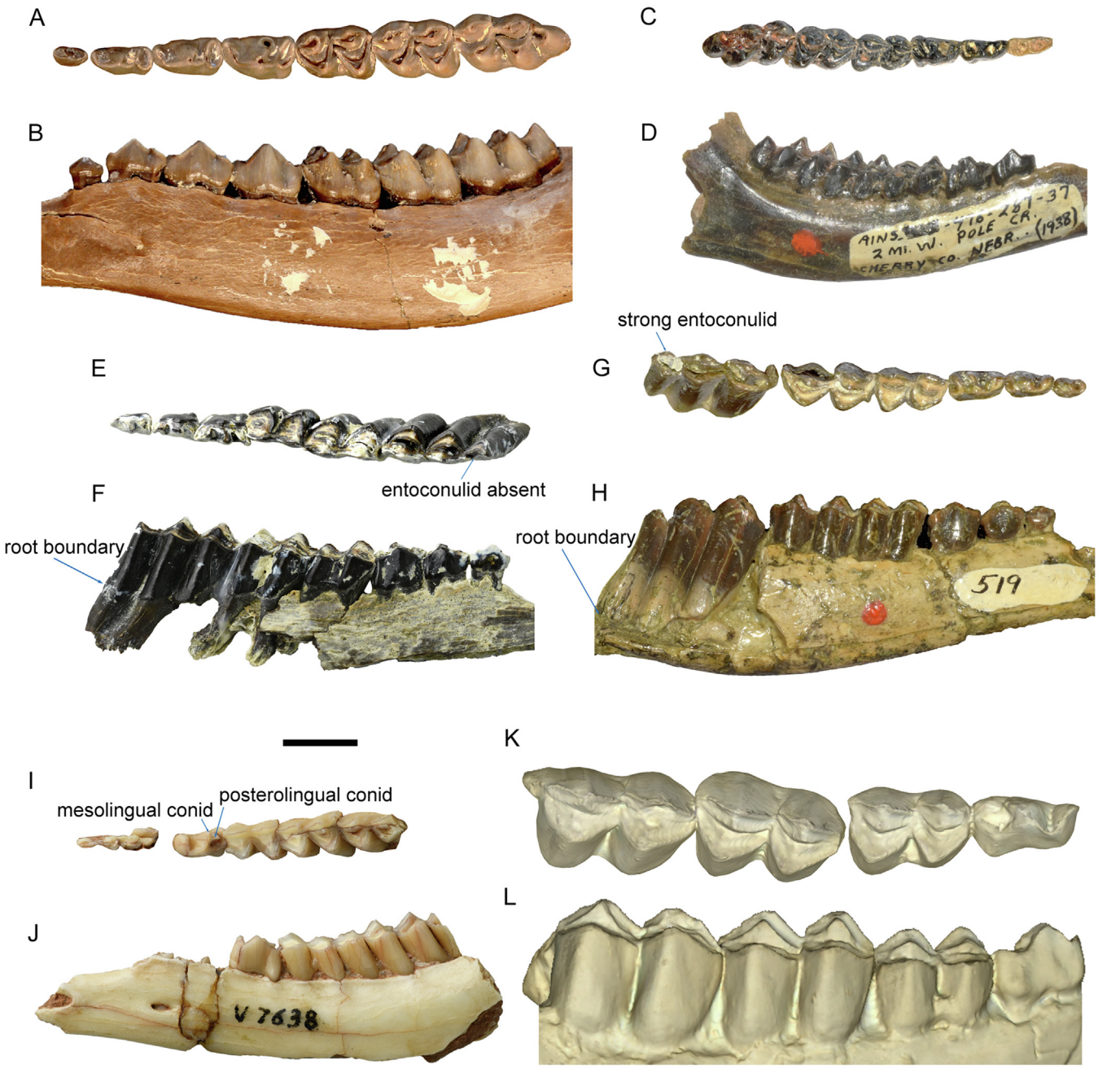

Fig. 5. Comparisons of lower tooth rows of selenodont artiodactyls. **A**, **B**. *Amphitragulus elegans*, a stem pecoran from the Agenian of Europe, NMB AM 7926, p1–m3. **C**, **D**. *Pseudoblastomeryx falkenbachi*, a blastomerycid pecoran from the Arikareean of North America, AM 31530, p3–m3. **E**, **F**. *Kubanotragus*? sp., a hypsodontine bovid from the Shanwangian of Central Asia, IVPP V33591, p2–m3. **G**, **H**. *Paracosoryx* sp., a merycodontine antilocaprid from the Barstovian of North America, AM 51960, p3–m3. **I**, **J**. "*Palaeohypsodontus* cf. *asiaticus*" a ruminant? from the Ulantatalian of East Asia, IVPP V7638, p4–m3. **K**, **L**. *Nothokemas* sp., a nothokemaline camelid from the Arikareean of North America, AM 99243 (cast), p4–m3. Specimens are in occlusal and buccal views. Scale bar: 10 mm.

dorcapolis nov. gen., nov. sp. In "*A.*" *feningrei*, the P2 and P3 lingual cones are centrally positioned, the metaconid and entoconid are laterally compressed and aligned, and the p4 lacks a pronounced anterior stylid – all contrasting with *L. dorcapolis* nov. gen., nov. sp. The size range of "*A.*" *feningrei* overlaps with that of *L. dorcapolis* nov. gen., nov. sp. (Fig. 4(A–C)).

Amphitragulus primaevus has been proposed as the ancestor of the type species *A. elegans*. Both species exceed *L. dorcapolis* nov. gen., nov. sp. in size (Fig. 4(A–C)). Similar to *Labrangomeryx* nov. gen., these "true" *Amphitragulus* taxa exhibit bunoselenodont cheek tooth morphology. The p4 of *L. dorcapolis* nov. gen., nov. sp. further parallels *A. primaevus* in retaining a non-distally oblique transverse cristid (distally oblique in *A. elegans*) and a robust anterior stylid (absent in *A. elegans*; Fig. 5(A, B)). However, *A. primaevus* and *A. elegans* (Fig. 5(A, B)) diverge from *L. dorcapolis* nov. gen., nov. sp. in exhibiting a weakly developed P2 lingual cone, absence of mesial displacement in the P3 lingual cone, rudimentary upper molar secondary structures (e.g., external postprotocrista), and an m3 posterior fossa characterized by a distal notch typically accompanied by a pronounced entoconulid.

Amphitragulus lemanensis may warrant assignment to a distinct genus based on its cervid-like double lacrimal orifices. Because Jehenne (1985) provisionally reclassified this species as *Hydropotopsis lemanensis* in his unpublished Ph.D. thesis, this nomenclatural proposal remains informal. Subsequent mentions by Ginsburg et al. (1991) in their faunal description of Barbotan-les-thermes constitute only a secondary citation of this unavailable name. Following current taxonomic standards, we maintain the original designation *Amphitragulus lemanensis* pending formal revision. Preliminary observations based on limited NMB material suggest *Amphitragulus lemanensis* exhibits heightened selenodonty in cheek tooth morphology compared to *A. elegans* and further diverges from *L. dorcapolis* nov. gen., nov. sp. Its size also surpasses that of *L. dorcapolis* nov. gen., nov. sp. (Fig. 4(A–C)).

Oriomeryx was erected for the reassignment of *Amphitragulus major*, with a second species, *O. willii* – originally attributed to *Palaeomeryx* aff. *kaupi* (Obergfell, 1957; Ginsburg, 1985). *Oriomeryx* represents a large-bodied genus (*O. willii* exceeding *O. major* in size) and exhibits marked morphological divergence from *L. dorcapolis* nov. gen., nov. sp., including: a robust lingual cingulum on P4, absence of a p4 anterior stylid contrasted by a prominent lingual groove, incomplete enclosure of the m3 back fossa, and a well-developed m3 entoconulid (Filhol, 1881; Viret, 1929).

Dremotherium constitutes the second key genus, serving as the morphological counterpart to *Amphitragulus*. Two species are recognized: the smaller Oligocene *D. guthi* (Jehenne, 1987) and the larger Miocene *D. feignouxi* (Filhol, 1881; Sigogneau, 1968; Viret, 1929; Costeur, 2011). Both species exceed *L. dorcapolis* nov. gen., nov. sp. in size. *Dremotherium* is unequivocally distinguished from *L. dorcapolis* nov. gen., nov. sp. by its heightened cheek tooth selenodonty. Additionally, *Dremotherium* exhibits: a weakly developed P2 lingual cone, a centrally positioned P3 lingual cone, a potential P4 lingual cingulum, a p4 with a distally oblique transverse cristid featuring a mesial buckle, and a pronounced posterolingual cristid – traits absent in *L. dorcapolis* nov. gen., nov. sp.

Bendenomeryx, another genus marked by extreme selenodonty, comprises three species: the Oligocene *B. milloquensis* and the Miocene *B. paulhiacensis* and *B. truyolsi* (Jehenne, 1988; Ginsburg et al., 1994). All three species substantially surpass *L. dorcapolis* nov. gen., nov. sp. in size. Morphologically, *Bendenomeryx* is characterized by mediolaterally expanded P2–P3 with enlarged lingual cones, yielding a subcircular occlusal outline. The lower molars trend toward a sub-ovoid shape. The p4 displays closely approximated mesolingual and mesolabial conids, resulting in an abbreviated transverse cristid. The m3 back fossa remains lingually open. Collectively, these features starkly contrast with *L. dorcapolis* nov. gen., nov. sp.

Andegameryx comprises three species: *A. andegaviensis*, *A. laugnacensis*, and *A. serum*. The first two species exceed *L. dorcapolis* nov. gen., nov. sp. in size, while *A. serum* approximates its dimensions (Fig. 4(A–C)). Although *Andegameryx* shares a relatively bunoselenodont dentition with *L. dorcapolis* nov. gen., nov. sp., it typically lacks an external postprotocristid (*Palaeomeryx*-fold; Ginsburg, 1971; Ginsburg and Morales, 1989; Ginsburg et al., 1991, 1994) – a key distinction. However, *A. serum* (Obergfell, 1957) uniquely retains this cristid. Despite this similarity, *A. serum* diverges from *L. dorcapolis* nov. gen., nov. sp. in its weakly developed P2 lingual cone, centrally positioned P3 lingual cone, rudimentary or absent metastylids, and simplified m3 third lobe morphology (Obergfell, 1957; Ginsburg, 1971; Ginsburg et al., 1991, 1994; Rössner, 1995; Quiralte and Morales, 2011).

Friburgomeryx wallenriedensis, a rare Early Miocene taxon (Becker et al., 2001; Mennecart et al., 2016), exhibits pronounced bunoselenodonty relative to contemporaneous forms. It differs from *L. dorcapolis* nov. gen., nov. sp. in its attenuated external postprotocristid, poorly molarized lower premolars, aligned metaconid-entoconid pair, and larger size.

Babameryx engesseri, an enigmatic latest Oligocene taxon, is distinguished from *L. dorcapolis* nov. gen., nov. sp. by a robust P4 lingual cingulum, reduced upper molar metaconule, presence of a metacone rib, weakly developed metastylid, and incomplete postentocristid.

In the latest Oligocene and earliest Miocene of Central and East Asia, hornless pecorans are exceptionally scarce in the fossil record. Vislobokova (1997) documented *Amphitragulus* cf. *quercyi*, *A.* cf. *gracilis*, and *A.* cf. *boulangeri* from Mongolia, alongside *Amphitragulus boulangeri* and *Amphitragulus* sp. from Kazakhstan. Additionally, she reported isolated molars attributed to *Amphitragulus boulangeri* from the Early Miocene Tagai locality near Lake Baikal, Russia (Vislobokova, 1994). While these dental elements exhibit morphological affinities with *L. dorcapolis* nov. gen., nov. sp. in crown morphology, critical premolar elements remain undocumented in the Tagai material. This absence of diagnostic anterior dentition precludes definitive taxonomic assignment. *Amphitragulus minoensis*, from the early Miocene Hiramaki Fm. (Japan), represents another regional record. Though substantially larger than *L. dorcapolis* nov. gen., nov. sp., its holotype exhibits extensive occlusal wear, limiting detailed morphological comparison (Nishioka et al., 2016). A further indeterminate cervoid specimen (Cervoidea fam., gen. et sp. indet.) from the coeval Koura Fm. (Japan) also exceeds *L. dorcapolis* nov. gen., nov. sp. in size, differing further in its moderately taller tooth crowns, absence of p1, and pronounced entoconid rib (Nishioka et al., 2016).

Several diminutive pecorans have been documented from the Late Oligocene to Early Miocene of Pakistan, including *Gelocus? gajensis*, *Prodremotherium? beatrix*, and *Bugtimeryx pilgrim* (Pilgrim, 1912; Ginsburg et al., 2001). Although Ginsburg et al. (2001) reclassified the former two within *Bugtimeryx* and posited its affinity as a stem giraffoid, the phylogenetic placement of these taxa remains provisional, warranting further study (Métais et al., 2017). All exceed *L. dorcapolis* nov. gen., nov. sp. in size. Key differential traits include: an attenuated or absent external postprotocristid (*Palaeomeryx*-fold), reduced metastylid, aligned metaconid-entoconid pair, and a distinct entoconulid on m3, demarcated from the hypoconulid (Barry et al., 2005) – features incongruent with *L. dorcapolis* nov. gen., nov. sp. Métais et al. (2017) additionally reported aff. *Amphitragulus* sp., *Mosaicomeryx* aff. *quercyi*, and *Paalitherium gurki* from the mid-Oligocene Paali-C2 locality (Dera Bugti). Among these, *L. dorcapolis* nov. gen., nov. sp. diverges from aff. *Amphitragulus* sp. in its more robust metastylid, from *Mosaicomeryx* aff. *quercyi* in retaining an external postprotocristid and abbreviated p3, and from *Paalitherium gurki* – an aberrant ruminant characterized by dual external postprotocristids

forming a V-shaped structure and a minor fork on the posthypocristid – in lacking such autapomorphies.

Hornless pecorans are also documented from the earliest Miocene of Africa. *Walangania*, a well-studied genus, exhibits marginally heightened selenodonty in its cheek teeth compared to *L. dorcapolis* nov. gen., nov. sp. The larger species, *W. africanus*, slightly exceeds *L. dorcapolis* nov. gen., nov. sp. in size and retains an attenuated external postprotocristid. The smaller species, *W. gracilis* – comparable in size to *L. dorcapolis* nov. gen., nov. sp. – lacks this cristid entirely (Whitworth, 1958). *Walangania* further diverges from *L. dorcapolis* nov. gen., nov. sp. in its reduced metastylids, aligned metaconid-entoconid pair, weakly developed upper molar secondary structures, and faint M3 lingual cingulum (Janis and Scott, 1987; Barry et al., 2005). Another taxon, "*Gelocus*" *whitworthi*, displays marked aberrance, notably a forked postentocristid and aligned metaconid-entoconid – distinct from *L. dorcapolis* nov. gen., nov. sp. Intriguingly, a pronounced enamel fold within the m3 back fossa parallels the condition observed in IVPP V33529, an isolated m3 of *L. dorcapolis* nov. gen., nov. sp. (Fig. 3(L, M)). We interpret this similarity as a non-diagnostic, incidental convergence.

In North America, hornless pecorans emerged abruptly during the late Arikareean (earliest Miocene), with *Problastomeryx primus* and *Pseudoblastomeryx falkenbachi* (Fig. 5(C, D)) appearing first, followed shortly by *Parablastomeryx gregorii* (Frick, 1937; Webb, 1998; Prothero, 2007, 2011). While these taxa diverge in body size and limb proportions (slenderness vs. robustness), their dental morphology is congruent. *Labrangomeryx dorcapolis* nov. gen., nov. sp. shares notable similarities with these North American taxa, particularly in size (Fig. 4(A–C)). In the upper dentition of the American taxa, the P2 and P3 exhibit prominent lingual cones, with the P3 cone moderately displaced mesially (though less pronounced than in *L. dorcapolis* nov. gen., nov. sp.). The parastyle, mesostyle, and paracone bear pronounced ribs, whereas metacone ribs are faint on M1–M2 and absent on M3. The metaconule is minimally reduced. The M3 anterolingual cingulum is less developed compared to *L. dorcapolis* nov. gen., nov. sp., and the external postprotocrista is typically absent (unlike *L. dorcapolis* nov. gen., nov. sp.), though minor enamel spurs occur within fossae. The lower molars of *Problastomeryx*, *Pseudoblastomeryx*, and *Parablastomeryx* are similarly brachydont-bunoselenodont, with marginally taller crowns than *L. dorcapolis* nov. gen., nov. sp. A p1 may variably persist or be absent. The p3 and p4 are proportionally elongate relative to *L. dorcapolis* nov. gen., nov. sp. The p4 retains a mesolingual conid and a weakly oblique transverse cristid. An external postprotocristid is present but attenuated, and the metastylid is moderately developed. The m1–m2 display narrow notches at the mesio- and distolingual corners, resulting from proximate but non-convergent cristid termini. The m3 back fossa forms a complete ring, with a rudimentary entoconulid.

Based on our comparative analysis, *Labrangomeryx dorcapolis* nov. gen., nov. sp. exhibits a unique combination of morphological features that justify its recognition as a distinct genus. Furthermore, *L. dorcapolis* nov. gen., nov. sp. shares notable similarities with the European *Pomelomeryx boulangeri* and "*Amphitragulus*" *quercyi*, and demonstrates strong affinities to North American taxa such as *Problastomeryx*, *Pseudoblastomeryx*, and *Parablastomeryx*. These relationships suggest potential evolutionary connections between Eurasian and North American pecorans, which are further explored in the cladistic analysis presented below.

Additionally, the cheek teeth morphology of *L. dorcapolis* nov. gen., nov. sp. diverges significantly from early Cervidae and Moschidae, characterized by its pronounced brachydont-bunoselenodont structure. Unlike any known cervid or moschid, the p4 of *L. dorcapolis* nov. gen., nov. sp. only bears a small mesolingual conid with a rudimentary posterolingual cristid (p4 anterolingual cristid is present in Moschidae, and p4 posterolingual cristid is well-developed in Cervidae), and the m3 entoconulid is nearly absent (isolated in Cervidae, and sharp-apex-like in Moschidae), resulting in a ring-like back fossa. Therefore, attributing *L. dorcapolis* nov. gen., nov. sp. to either Cervidae or Moschidae appears unlikely based on these distinctive dental traits.

Genus ***Sinopalaeoceros*** Chen, 1988.

Type and only species: *Sinopalaeoceros xiejiaensis* (Li and Qiu, 1980).

Occurrence: Early Miocene (MN 1–3), northern China.

Emended diagnosis: High-crowned cheek teeth (m2 height/width ratio approximately 3), p4 with four oblique cristids (anterior conid, transverse cristid, posterolingual conid, and posterolingual stylid, mesially to distally) originating from the buccal wall, with the distal two cristids enclosing the back valley. Lingually, sharp-apexed lingual conids and thin, prominent stylid ribs. m3 with a pronounced entoconulid and closed back fossa. Ectostylid absent. Differing from all hornless pecorans in high tooth crown and mesial inclination of m3 in lingual view. Differing from hypsodontine bovids (*Kubanotragus*, *Turcoceros*, *Hypsodontinus*) in mesial inclination of m3 in lingual view, presence of a strong m3 entoconulid, and typically higher tooth crown. Differing from merycodontine antilocaprids in smaller size and lesser hypsodonty. Differing from tragulids and cameloids in p4 having four oblique cristids derived from a buccal wall.

Sinopalaeoceros xiejiaensis (Li and Qiu, 1980)

Fig. 6

1980. *Oioceros* (?) *xiejiaensis* nov. sp. – Li and Qiu, p. 208, pl. 1, figs. 8, 9.

1988. *Sinopalaeoceros xiejiaensis* (Li and Qiu) – Chen, p. 166.

Holotype: IVPP V6007, a right upper jaw with M2 and M3.

Paratypes: IVPP V6008, a left upper jaw with M1 and M2, a right DP4 (originally identified as an M1), a right M2, and a left lower jaw with m1 and m2.

Material (from the Shaoma locality): IVPP V33533, a right lower jaw with m2 and m3; V33534, a left p4; V33535, a left M1 and M2; V33536, a right P2.

Type locality and horizon: Xiejia (IVPP 78027), Xining City, Qinghai Province, China.

Occurrence: Early Miocene (MN 1–3), northern China.

Measurements: See Table 1.

Diagnosis: As for the genus, by monotypy.

Descriptions:

The P2 (IVPP V33536; Fig. 6(A–C)) is moderately high, with a straight buccal wall and a rounded lingual wall. The posterior lingual cone is circular, featuring a deep anterior groove that outlines a slightly defined anterolingual cone. The mesial edge of the tooth is rounded and bears a weak anterior style. The labial cone remains undivided and exhibits a buccal angle. The distal end of the tooth shows a sharp corner, bearing a distally oriented posterior style. Each crista is nearly invisible due to extensive wear. In buccal view, the ribs of the labial cone, as well as the anterior and posterior styles, are columnar and parallel.

The M1 is severely broken (not photographed), whereas the M2 is complete (IVPP V33535; Fig. 6(D–F)). The M2 exhibits moderate wear and a high tooth crown. The first lobe is relatively short and wide, while the second lobe is long and relatively narrow. The protocone is triangular with a distinct lingual angle. The preprotocrista merges with the preparacrista to form a moderately developed, mesobuccally oriented parastyle. The postprotocrista curves and joins the mesial wall of the premetaconulecrista. The paracone is inflated on both the lingual and buccal sides, featuring a blunt buccal angle. The postparacrista is slightly curved and meets the premetacrista at the moderately developed mesostyle.

Fig. 6. *Sinopalaeoceros xiejiaensis* from the Shaoma (A–L) and Xiejia (M–AA) fossil localities. **A–C**. IVPP V33536, right P2. **D–F**, IVPP V33535, left M2. **G–I**. V33534, left p4. **J–L**. IVPP V33533, right m2 and m3. **M–O**. IVPP V6007, right M1 and M2, type specimen. **P–R**. IVPP V6008, left M1 and M2. **S–U**, IVPP V6008, right DP4. **V–X**. IVPP V6008, right M2. **Y–AA**, IVPP V6008, left m1 and m2. Specimens are in occlusal, lingual, and buccal views. Scale bar: 10 mm.

The metacone lacks inflation and extends slightly obliquely relative to the paracone. The metaconule is triangular, also bearing a blunt buccal angle, positioned more buccally than the protocone. The premetaconulecrista merges with the postprotocrista near the lingual wall of the postparacrista, nearly fusing with it. The postmetaconulecrista is elongated and joins the postmetacrista, forming a strong, buccally oriented metastyle. In buccal view, the ribs of the parastyle, mesostyle, metastyle, and paracone are pro-

nounced, whereas the metacone rib is very weak. These ribs run nearly parallel for most of their length but converge close to the root. The ribs of the parastyle and paracone fuse into one at the base.

The p4 (IVPP V33534; Fig. 6(G–I)) is moderately high, relatively long and narrow, with thin cristids. The anterior conid is nearly perpendicular to the median axis, only slightly oblique, and lacks an anterior stylid. The mesolabial conid is slightly swollen and bears a long, thin anterolabial cristid and a posterolabial cristid. The transverse cristid is strongly distally oblique, and its distal end is almost not inflated, making the mesolingual conid indistinguishable in initial wear stages. However, the distal end of the transverse cristid gradually expands from the crown towards the root. The posterolabial conid is slightly lingually curved and radiates a posterolingual conid and a posterior stylid that link to each other distally, forming a narrow, oblique ring.

The m2 (IVPP V33533; Fig. 6(J–L)) is in deep wear and has a high tooth crown. The trigonid is so deeply worn that the anterior fossa is vanished. In this wearing state, the trigonid is pentagonal with a buccal angle. The entoconid is slightly inflated with short pre- and postentocristids. The metastylid has been worn out, but the entostylid is present. The hypoconid is triangular with a sharp buccal angle. The anterior cingulid has been worn out, and no ectostylid is present. In lingual view, the metaconid and entoconid are high and sharp. The ribs of the mesostylid and entostylid are sharp and thin, while those of the metaconid and entoconid are blunt and weak. The metastylid rib is absent.

The m3 (IVPP V33533; Fig. 6(J–L)) is high-crowned and laterally compacted, with very narrow fossae. The three lobes are well defined. The metaconid is only slightly inflated and has a curved premetacristid. The mesostyle is prominent, while the metastyle is small and attaches to the middle of the postmetacristid. The protoconid has a blunt triangular buccal angle and extends a long, curved preprotocristid that joins the premetacristid. The short postprotocristid meets the postmetacristid and preentocristid, forming a "T"-shape junction. The entoconid is aligned with the metaconid and is slightly inflated with short pre- and postentocristids. The hypoconid is similar to the protoconid, showing a blunt triangular buccal angle. The prehypocristid is curved and reaches the lingual wall of the preentocristid. The posthypocristid meets the postentocristid, closing the posterior fossa. An entostylid is absent. Both the entoconulid (broken at the tip) and the hypoconulid are well-developed with complete cristids that enclose the back fossa. A strong anterior cingulid is present, and ectostylid and posterior ectostylid are absent. In lingual view, the metaconid and entoconid are high and sharp (the tip of the entoconulid is broken). The ribs of the mesostylid and metastylid are thin and slightly converge, while the ribs of the metaconid, entoconid, and entoconulid are blunt and weak. Overall, the m3 shows a mesial inclination from the occlusal plane, as evidenced by the oblique orientations of the ribs.

Remarks: The present material represents a small pecoran with a high tooth crown. The overall morphology closely matches that of *Sinopalaeoceros xiejiaensis*, a representative taxon from the Xiejian Stage. Due to the unclear photos in the original plate, we have included type specimens from Xiejia (Fig. 6(M–AA)) alongside the new specimens from Shaoma for comparison. Additionally, we reidentified Fig. 6(S–U) (one specimen of IVPP V6008) as a DP4 rather than an M1, due to its significantly lower crown height. The new specimens are identical to the type material both in size and morphology, except for the slightly weaker metastylid, which appears to be caused by deeper wear.

Sinopalaeoceros xiejiaensis, originally referred to as *Oioceros*? *xiejiaensis*, was previously classified as a bovid (Li and Qiu, 1980; Chen, 1988). However, no horncore has been discovered from such early strata. Small hornless ruminants with a high tooth crown have been previously reported from the Oligocene and Early Miocene of Asia, including *Palaeohypsodontus asiaticus*, *P. zinensis*, *Hanhaicerus qii*, *Gobiocerus mongolicus*, and some other materials referred to as Bovidae indet. (Sokolov, 1952; Trofimov, 1958; Huang, 1985; Métais et al., 2003). Furthermore, *Namibiomeryx senuti* is a hornless pecoran from the Early Miocene of Africa (Morales et al., 1995).

Palaeohypsodontus asiaticus was reported from Tatal Gol and Hsanda Gol, Late Oligocene of Mongolia. Compared to *S. xiejiaensis*, *P. asiaticus* was smaller and relatively lower crowned. The m3 is not mesially inclined in lingual view, unlike that of *S. xiejiaensis*. *Palaeohypsodontus zinensis* was reported from the Late Oligocene of Dera Bugti, South Asia (Métais et al., 2003). It is larger and higher-crowned than *P. asiaticus*, but is still lower-crowned compared to *S. xiejiaensis* (Fig. 4(D–F)). The unaligned proximal and distal pulley of the astragalus renders the pecoran affinity of *Palaeohypsodontus* questionable. However, "*Palaeohypsodontus* cf. *asiaticus*" from Ulantatal, Early Oligocene of China (Fig. 5(I, J)), is much larger and lower-crowned (Fig. 4(D–F)). The lower molars are wider than those of *S. xiejiaensis*. The anterior cingulid is absent. The p4 possesses thick cristids with an isolated posteriolingual conid that joins the transverse cristid. This morphology is more or less tragulid-like or camelid-like (Fig. 5(I–L)), rather than pecoran-like. *Hanhaicerus qii* was from the same locality as *P.* cf. *asiaticus*. It is even larger and lower-crowned (Fig. 4(D–F)). The metastylids are pronounced and the entoconulid and hypoconulid do not close the distal end of the back fossa. The anterior cingulid is also absent. *Gobiocerus mongolicus* is from the Loh Fm. of Hsanda Gol, Early Miocene (Sokolov, 1952). The m1 and m2 are much larger than those of *S. xiejiaensis*, but relatively lower-crowned. It is possibly a bovid closely related to *Hypsodontus* or *Turcocerus*, belonging to the Hypsodontinae of Bovidae. Vislobokova and Daxner-Höck (2002) reported ?*Gobiocerus* sp. from C1 zone, but its assignment to this genus is questionable. *Namibiomeryx senuti* is slightly smaller than *S. xiejiaensis*. The tooth morphology of *N. senuti* is close to that of *H. qii*, such as the relatively low tooth crown (Fig. 4(D–F)) and thicker ribs of stylids. Particularly, the posterior fossa is open due to the disconnection of the postentocristid and posthypocristid. The m3 back fossa is highly notched (Morales et al., 1995). The above taxa are all distinct from *S. xiejiaensis*.

Blastomeryx, *Machaeromeryx*, and *Longirostromeryx* are hornless ruminants from North America, with later occurrences than *S. xiejiaensis*. Although the tooth crowns have increased (compared with *Problastomeryx*, *Pseudoblastomeryx*, and *Parablastomeryx*) in the former taxa, they are still markedly lower than those of *S. xiejiaensis* (Frick, 1937; Webb, 1998).

Although *S. xiejiaensis* was previously regarded as a bovid, its tooth morphology differs significantly from that of early-middle Miocene bovids. The early Bovinae, like *Eotragus*, have relatively low tooth crowns, which are very different from those of *S. xiejiaensis* (Made, 2012). Further comparisons with the high-crowned Hypsodontinae, such as *Hypsodontus*, *Turcocerus*, and *Kubanotragus*, reveal that in these taxa, the third lobe of m3 only has a hypoconulid, missing an entoconulid (therefore, the m3 back fossa is absent in Hypsodontinae; Köhler, 1987; Fig. 5(E, F)). The ectostylid and entostyle may be present in Hypsodontinae (absent in *S. xiejiaensis*). The m3 is not mesially inclined in lingual view because the occlusal surface of Hypsodontinae is perpendicular to the m3 vertical axis. The mesially inclined m3 of *S. xiejiaensis* appears to correlate with its extremely hypsodont nature, which is larger than that of the Hypsodontinae (Fig. 4(F)). In fact, the cheek tooth height of *S. xiejiaensis* is larger than any early-middle Miocene ruminants except for the merycodontines of Antilocapridae (Fig. 4(D–F)), as previously mentioned (Janis and Manning, 1998). In merycodontines, such as *Merycodus*, *Paracosoryx*, and *Merriamoceros*, except for the larger size, there is almost no difference between *S. xiejiaensis*

and merycodontines in lower cheek tooth morphology (Fig. 5(G, H)), including the hypsodonty level. However, the upper cheek teeth of merycodontines may be even higher than those of *S. xiejiaensis*, but with similar tooth morphology (Frick, 1937).

Ruminantia gen. et sp. indet.
Fig. 7(A–J)

Material: IVPP V33537, a right metacarpal III-IV, distal ends unfused; IVPP V33538, a distal end of left metacarpal III-IV; IVPP V33539, a distal epiphysis of a metatarsus.

Description:

The complete metacarpal III-IV, IVPP V33537 (Fig. 7(A–E)), is semicylindrical and moderately elongated. In dorsal view, a shallow groove runs along the median axis. In volar view, the groove for flexor tendons is wide and shallow, gradually vanishing distally. In lateral view, there is a weak impression for the lateral extensor tendon. In proximal view, the fan-shaped dorsomedial facet for the magnum occupies most of the surface. A sub-square volomedial facet for the trapezoid is relatively large and meets the magnum facet by a relatively long crest. The fan-shaped lateral facet for

Fig. 7. Pecora gen. et sp. indet. (A–J) and Protoceratidae? gen. et sp. indet. (K–M) from the Shaoma fossil locality (Gansu, China). **A**–**E**. IVPP V33537, right metacarpal III-IV, in proximal (A), dorsal (B), volar (C), medial (D), and lateral (E) views. **F**–**H**. IVPP V33538, left metacarpal III-IV, in dorsal (F), volar (G), and distal (H) views. **I**, **J**. IVPP V33539, distal epiphysis of a metatarsus?, in volar (I) and abaxial (J) views. **K**–**M**. IVPP V33554, left p4, in occlusal (K), lingual (L), and buccal (M) views. Notes: 1, facet for magnum; 2, step between facets for magnum and unciform; 3, facet for unciform; 4, facet for trapezoid; 5, bony bridge of gully; 6, incomplete pulley; 7, open gully; 8, facets for MC II; 9, facets for MC V; 10, groove between mesolabial and posterolabial conids. Scale bar: 10 mm.

the unciform is smaller and lower positioned than the magnum facet, meeting the latter by a small step. The proximomedial facet for the metacarpal II is relatively large, while that for the metacarpal V at the proximolateral facet is small. Measurements (in mm): preserved length, 78.49; proximal width, 12.09; proximal thickness, 8.43; middle shaft width, 8.11; middle shaft thickness, 5.84.

In the distal part of IVPP V33537, the distal bony bridge has not been formed (Fig. 7(A–E)). We do not know if the bridge would be formed in the adult stage. In IVPP V33538 (Fig. 7(F–H)), a complete bony bridge is formed, with tightly fused distal pulleys. However, the distal keel of each pulley is incomplete, as the dorsal part is poorly developed. Measurements (in mm): preserved length, 21.59; distal width, 12.40; distal thickness, 7.58.

IVPP V33539 (Fig. 7(I, J)) is a distal unfused pulley, identified as part of a metatarsus III-IV due to its relatively large dorsoplantar dimension. The dorsal part of the distal keel is also poorly developed. Measurements (in mm): length, 8.86; width, 6.68; thickness, 8.25.

The above metapodial specimens may belong to either *Labrangomeryx dorcapolis* nov. gen., nov. sp. or *Sinopalaeoceros xiejiaensis*. There are several primitive features in the specimens, including the incomplete metapodial distal keel and the large trapezoid facet (indicating that the trapezoid possibly has not been fused with the magnum), compared with higher pecorans (Janis and Scott, 1987)

Tylopoda? Illiger, 1811
Protoceratidae? Marsh, 1891
Protoceratidae? gen. et sp. indet.
Fig. 7(K–M)

Material: IVPP V33554, a left p4 (Fig. 7(K–M)).

Measurements: See Table 1.

Description: The tooth is very large, with a sub-triangular occlusal shape. The enamel is thick. The mesolabial cone is elliptical and extends mesiolingually-distolabially. The anterolabial cristid is very thick and runs along the mesiobuccal margin, showing a pronounced posterolabial groove. A circular anterior conid is separated from the distolingual side of the mesiobuccal tip. The mesolingual conid is slightly broken and stands along the lingual side of the mesolabial conid. A posterolingual cristid extends distally. The posterolabial conid is large and slightly transversely expanded. A thick, straight posterolabial cristid directly connects the mesolabial and posterolabial conids. A small posterolingual conid sits at the distolingual corner of the tooth.

Remarks: The huge size is greater than that of any taxon of Tragulidae at that time, and usually, the contour of p4 in tragulids is relatively long and narrow (Whitworth, 1958; Qiu and Gu, 1991; Ginsburg et al., 2001). On the other hand, this specimen shows characters of some North American camelids of Arikareean, like *Nothokemas* and *Aguascalientia* of Camelidae (Rincon et al., 2012; Marriott et al., 2022) and the protoceratids, *Syndyoceras* and *Paratoceras* (Patton and Taylor, 1973). Considering the low crown, we provisionally refer to it as Protoceratidae? gen. et sp. indet. This attribution remains highly tentative and requires verification through additional material.

3.2. Cladistic analysis

Our cladistic analysis elucidates early differentiation patterns among ruminant families through an expanded morphological matrix derived from Mennecart and Métais (2015), incorporating 39 ruminant taxa (including representatives of all crown families) with *Amphirhagatherium weigelti* (Choeropotamidae) and *Merycoidodon culbertsoni* (Merycoidodontidae) as outgroups. Parsimony analysis generated two equally most parsimonious trees (length = 176; CI = 0.426; RI = 0.730), with the strict consensus tree's proximal topology mirroring previous work while revealing novel evolutionary relationships (Fig. 8). Basally positioned *Archeomeryx optatus* gives way to a trifurcation among *Miomeryx altaicus*, North American Tragulina (Hypertragulidae + Leptomerycidae), and a Eurasian clade comprising Tragulina-Pecora 'hybrids', where extant Tragulidae emerge derived post-Lophiomerycidae/"Gelocidae". Post-latest-Oligocene taxa (excluding *Gobiomeryx dubius* and *Pseudomeryx gobiensis*, whose positions remain tentative due to morphological incompleteness) form two well-defined monophyletic groups: One clade unites Late Oligocene-Early Miocene small brachydonts, in which *Labrangomeryx dorcapolis* nov. gen., nov. sp. is clustered with North American Blastomerycidae, supported by at least one synapomorphy: molars with strong metastylids (character 24; Texts S1, Appendix A [the same below]), and another two synapomorphies on the cladogram, MC V and MT II not fused with corresponding cannon bones (37, 43) is unknown in *Labrangomeryx* nov. gen. They further clustered with Eurasian taxa including *Dremotherium* spp., *Pomelomeryx gracilis*, and *Amphitragulus* spp. *Labrangomeryx dorcapolis* nov. gen., nov. sp. is unique in the following autapomorphies: P3 lingual cone anteriorly positioned (6), molar lingual cingulum only present on M3 (8), possible absence of complete distal metapodial keels (41). Another clade positions *Sinopalaeoceros xiejiaensis* basally within crown Pecora, clustering with primitive Antilocapridae (*Paracosoryx wilsoni*), supported by the following synapomorphies: p4 posterolingual cristid (19) and p4 mesolingual conid (21) missing; m3 third lobe possessing double apex (29), and very high cheek tooth crown (30). Interestingly, the Central Asian Oligocene taxa (*Gobimeryx* and *Pseudomeryx*) are clustered with *Sinopalaeoceros* + Antilocapridae. This topology further corroborates Morales et al. (1996) identification of *Andegameryx*/*Namibiomeryx* as Bovidae stem taxa, which alongside crown Giraffidae (*Canthumeryx sirtensis*) form a sister group to (Antilocapridae + *Sinopalaeoceros*), while Moschidae and Cervidae occupy more basal positions, contradicting the topology of molecular phylogeny (Hassanin et al., 2012; Chen et al., 2019); Palaeomerycidea are positioned outside of the Moschidae and Cervidae, not grouped with Giraffidae as Sánchez et al. (2015) demonstrated. These disparities may be caused by the more conservative check tooth characters in Palaeomerycidea, Cervidae, and Moschidae. These families were grouped in Cervoidea by Janis and Scott (1987). Nevertheless, in this analysis, *Labrangomeryx dorcapolis* nov. gen., nov. sp. is positioned as a stem Pecora, while *Sinopalaeoceros xiejiaensis* falls into the crown Pecora.

4. Discussion

Stem pecorans may have originated from the Early Oligocene of Eurasia, shortly after the Mongolian Remodeling event (Meng and McKenna, 1998). However, this hypothesis has been heavily debated. The increasing aridification and expansion of open environments in Asian inland areas appear to represent the primary driving forces behind the origin of pecorans in this region (Li et al., 2018). The Oligocene–Miocene transition marks an important stage in the early radiation of pecorans (Mennecart, 2012). During this period, pecorans dispersed into Africa and North America. However, East and Central Asia, as potential evolutionary centers for pecorans, exhibit notably incomplete fossil records. This situation may be partially attributed to the relatively limited fossil-bearing strata of this age in the region. More critically, it often stems from less thorough description and comparison, where specimens are typically assigned to Cervidae indet. or Bovidae indet. based solely on cheek tooth crown height.

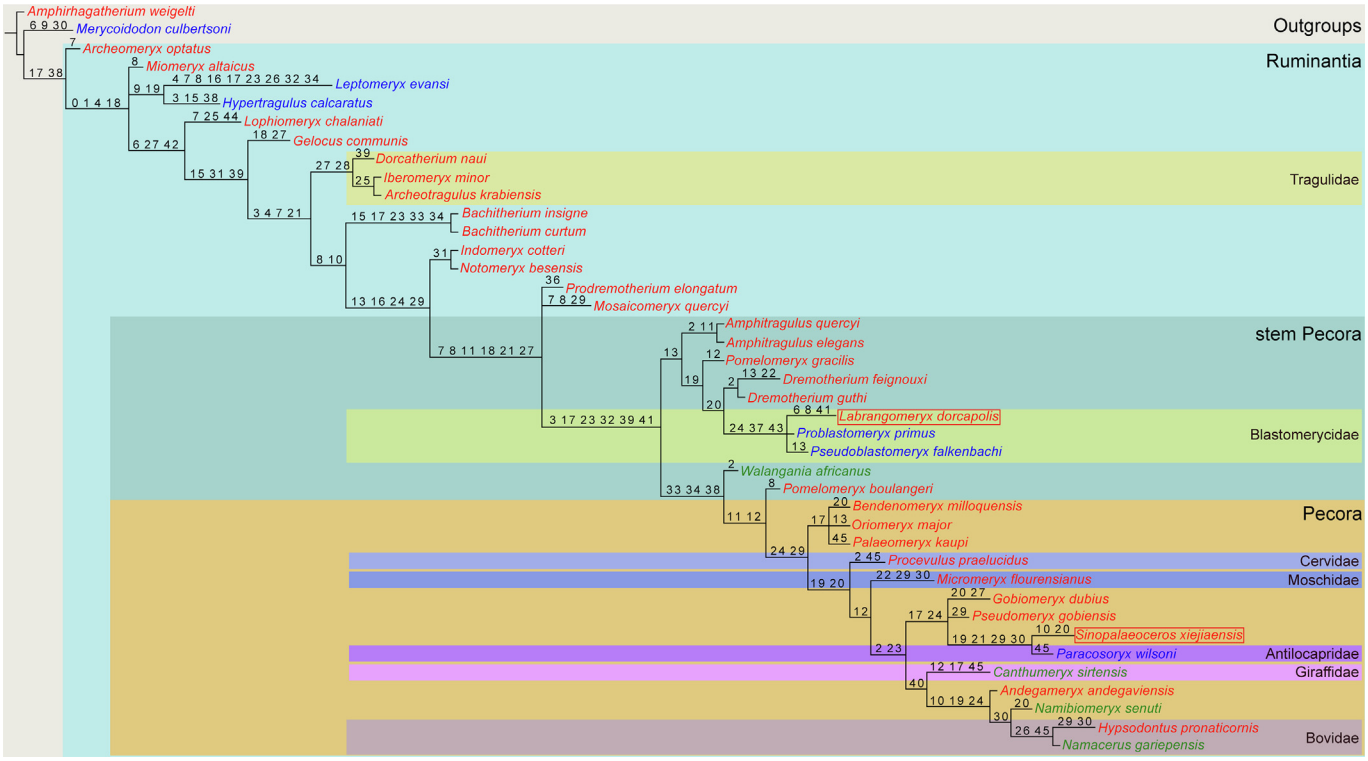

Fig. 8. Strict consensus tree resulting from the two MPTs of ruminants. Taxon name in Red: Eurasian; Blue: North American; Green: African. The numbers represent synapomorphic characters (Text S1; Appendix A) at each node. *Labrangomeryx dorcapolis* nov. gen., nov. sp. and *Sinopalaeoceros xiejiaensis* are marked in red rectangles.

The new ruminants from the Shaoma Locality provide an opportunity to advance understanding of the evolutionary history of crown pecoran families. Extant crown pecoran families (Antilocapridae, Giraffidae, Cervidae, Bovidae, and Moschidae) are united by their distinctive cranial appendages (except Moschidae, which lack such structures; Davis et al., 2011). The fossil record of these families emerged abruptly at ca. 20–19 Ma, appearing concurrently in Eurasia, Africa, and North America, and no cranial appendages have been documented prior to this age. If the presence of each distinct cranial appendage type is interpreted as a synapomorphy defining each pecoran family, earlier fossils cannot be confidently assigned to these crown families unless corresponding cranial appendages are preserved in the fossil record.

Our phylogenetic reconstruction based on morphological data suggests the potential relationship of ruminants between China and North America in the Early Miocene (Fig. 8). However, it contradicts the updated molecular phylogeny, in which Antilocapridae and Giraffidae represent the earliest diverging pecoran lineages, followed by Cervidae, and finally Moschidae and Bovidae (Hassanin et al., 2012; Chen et al., 2019). Within the molecular phylogenetic cladistic framework, hypsodonty evolved at least twice independently in crown pecorans – once in antilocaprids and bovids – and potentially also in certain giraffoids and cervids. High-crowned cheek teeth are a problematic synapomorphic trait for grouping fossil taxa, as hypsodonty also evolved independently in tylopods. The moderate hypsodonty of "*Palaeohypsodontus* cf. *asiaticus*" from Ulantatal could plausibly align it with Bovidae, Antilocapridae, or Camelidae (Fig. 5(I–L)). However, its p4 morphology more closely resembles camelids than pecorans or it can be further comparable with any selenodont artiodactyl family of mesodonty. Consequently, *Sinopalaeoceros xiejiaensis* cannot be definitively assigned to Bovidae or Antilocapridae; instead, it is better interpreted as a stem pecoran. The phylogenetic relationship of *S. xiejiaensis* with *Palaeohypsodontus* and *Hanhaicerus* remains unresolved, as these taxa exhibit non-pecoran traits (Métais et al., 2003). Similarly, low tooth crowns should not be used to group taxa with cervids, as this represents a plesiomorphic condition. *Labrangomeryx dorcapolis* nov. gen., nov. sp., with its brachydont and bunoselenodont cheek teeth, clearly occupies a more primitive evolutionary position relative to Cervidae and Moschidae. In our view, these early pecorans are best classified as stem groups, avoiding premature assignment to extant families. The isolated p4 provisionally referred to as Protoceratidae? gen. et sp. indet. is too large to belong to any contemporaneous traguline. Its tentative attribution to Protoceratidae remains speculative and necessitates verification through additional material. Nevertheless, its morphology aligns more closely with North American selenodont taxa than with endemic Asian groups.

5. Conclusions

In this article, we describe two newly discovered ruminants from the Shaoma locality of the earliest Miocene (Xiejian Age) in Gansu Province: *Labrangomeryx dorcapolis* nov. gen., nov. sp., and *Sinopalaeoceros xiejiaensis*. *L. dorcapolis* nov. gen., nov. sp. represents the first named low-crowned ruminant from the Xiejian Age of China, characterized by a unique combination of bunoselenodont features including a distinct labial cone on P2, a mesially shifted labial cone on P3, well-developed secondary structures (e.g., external postprotocrista, enamel spurs, and fossae folds), a pronounced anterolingual cingulum on M3, a p4 with a bifurcated anterior conid and a moderately developed mesolingual conid bearing a rudimentary posterolingual cristid, lower molars with unaligned metaconid and entoconid, moderate to strong metastylid and external postprotocristid, and an m3 with a ring-like back fossa lacking an entoconulid. Morphologically, *L. dorcapolis* nov.

gen., nov. sp. bridges Eurasian and North American pecorans, sharing affinities with European taxa (*Pomelmeryx boulangeri* and "*Amphitragulus*" *quercyi*) and North American taxa (*Problastomeryx primus*, *Pseudoblastomeryx falkenbachi*, and *Parablastomeryx gregorii*), a connection further supported by phylogenetic analysis. Its brachydont-bunoselenodont dentition and absence of antlers preclude classification within Cervidae or Moschidae. Meanwhile, *Sinopalaeoceros xiejiaensis*, previously misattributed to Bovidae due to its high hypsodonty, more closely resembles merycodontine antilocaprids but lacks cranial appendages, leading us to reclassify it as a stem pecoran. While Protoceratidae? gen. et sp. indet. shares some features with North American camelids and protoceratids (*Syndyoceras*, *Paratoceras*), its phylogenetic placement remains tentative. The new fossils from the Shaoma locality underscore the challenges of assigning Early Miocene fossils to crown families without cranial appendages, emphasizing the need for cautious interpretation of hypsodonty as a homoplastic trait. These findings highlight the evolutionary complexity of stem pecorans in Asia, where incomplete fossil records and reliance on dental characters complicate taxonomic assignments, urging renewed focus on cranial morphology and biogeographic context to resolve early pecoran radiations.

Declaration of generative AI and AI-assisted technologies in the writing process

During the preparation of this work the authors used Geogpt in order to improve English. After using this tool/service, the authors reviewed and edited the content as needed and take full responsibility for the content of the publication.

CRediT authorship contribution statement

Shi-Qi Wang: Writing – review & editing, Writing – original draft, Validation, Supervision, Methodology, Investigation, Funding acquisition, Data curation, Conceptualization. **Tao Deng:** Writing – review & editing, Validation, Supervision, Investigation, Funding acquisition. **Tingjiang Peng:** Writing – review & editing, Data curation, Conceptualization. **Bian Wang:** Writing – review & editing, Methodology, Investigation. **Qigao Jiangzuo:** Methodology, Conceptualization. **Jiao Fu:** Investigation, Data curation. **Danhui Sun:** Methodology, Data curation. **Luda Xing:** Data curation.

Data availability

No data was used for the research described in the article.

Declaration of competing interest

The authors declare that they have no known competing financial interests or personal relationships that could have appeared to influence the work reported in this paper.

Acknowledgements

We thank Wenyu Wu for preliminary identification of small mammals. We thank Jin Meng (AMNH) and Loic Costeur (NMB) for accessing comparative materials. We thank the two reviewers, Grégoire Métais and Loic Costeur, for many constructive suggestions to improve the manuscript. We thank Wanma Dangzhi and Gesang Ji, the government of the Hezuo City, for they support in the fossil excavation. We thank Wei Gao (IVPP) for taking photos. We thank Lu Li, Qinqin Shi, Jiao Ma, Shijie Li, Shaoguang Zhang, Sijian Xu, Chao Suo (IVPP) for participating in field works. The work was supported by the National Key Research and Development Program of China (No. 2023YFF0804501) and National Natural Science Foundation of China (42430207, 42472004).

Appendix A. Supplementary information

Supplementary information (including Texts S1, S2, Data S1 and Code S1) associated with this article can be found, in the online version, at: https://doi.org/10.1016/j.geobios.2025.06.002.

References

Bärmann, E.V., Rössner, G.E., 2011. Dental nomenclature in Ruminantia: towards a standard terminological framework. Mammalian Biology 76, 762–768.
Barry, J.C., Cote, S., MacLatchy, L., Lindsay, E.H., Kityo, R., Rajpar, A.R., 2005. Oligocene and Early Miocene ruminants (Mammalia, Artiodactyla) from Pakistan and Uganda. Palaeontologia Electronica 8, 22A.
Becker, D., Rössner, G.E., Picot, L., Berger, J.P., 2001. Early Miocene ruminants of Wallenried (USM, Aquitanian/Switzerland): sedimentology, biostratigraphy and paleoecology. Eclogae Geologica Helvetiae 94, 547–564.
Chen, G.F., 1988. Remarks on the *Oioceros* species (Bovidae, Artiodactyla, Mammalia) from the Neogene of China. Vertebrata PalAsiatica 26, 157–172 (in Chinese with English summary).
Chen, L., Qiu, Q., Jiang, Y., Wang, K., Lin, Z.S., Li, Z.P., Bibi, F., Yang, Y.Z., Wang, J.H., Nie, W.H., Su, W.T., Liu, G.C., Li, Q.Y., Fu, W.W., Pan, X.Y., Liu, C., Yang, J., Zhang, C. Z., Yin, Y., Wang, Y., Zhao, Y., Zhang, C., Wang, Z.K., Qin, Y.L., Liu, W., Wang, B., Ren, Y.D., Zhang, R., Zeng, Y., da Fonseca, R.R., Wei, B., Li, R., Wan, W.T., Zhao, R. P., Zhu, W.B., Wang, Y.T., Duan, S.C., Gao, Y., Zhang, Y.E., Chen, C.Y., Hvilsom, C., Epps, C.W., Chemnick, L.G., Dong, Y., Mirarab, S., Siegismund, H.R., Ryder, O.A., Gilbert, M.T.P., Lewin, H.A., Zhang, G.J., Heller, R., Wang, W., 2019. Large-scale ruminant genome sequencing provides insights into their evolution and distinct traits. Science 364, 1152.
Costeur, L., 2011. A partial skull of *Dremotherium feignouxi* from the Aquitanian of France (MN2, Saint-Gérand-le-Puy, Allier). Acta Geologica Slovaca 3, 105–112.
Davis, E.B., Brakora, K.A., Lee, A.H., 2011. Evolution of ruminant headgear: a review. Proceedings of the Royal Society B 278, 2857–2865.
Filhol, H., 1881. Étude des mammifères fossiles de Saint-Gérand le Puy (Allier). Seconde Partie. Annales des Sciences Géologiques 11, 1–86.
Frick, C., 1937. Horned ruminants of North America. Bulletin of the American Museum of Natural History 69, 1–669.
Ginsburg, L., 1971. Un ruminant nouveau des faluns Miocènes de la Touraine et de l'Anjou. Bulletin du Muséum d'histoire Naturelle 42, 996–1002.
Ginsburg, L., 1985. Systématique et évolution du genre Miocène *Palaeomeryx* (Artiodactyla Giraffoidea) en Europe. Comptes Rendus de l'Academie des Sciences, Sér. II: Mecanique-Physique-Chimie Sciences de l'Univers Sciences de la Terre 301, 1075–1078.
Ginsburg, L., de Broin, F., Crouzel, F., Duranthon, F., Escuillié, F., Juillard, F., Lassaube, S., 1991. Les Vertébrés du Miocène inférieur de Barbotan-les-Thermes (Gers). Annales de Paléontologie 77, 161–216.
Ginsburg, L., Morales, J., 1989. Les ruminants du Miocène inférieur de Laugnac (Lot-et-Garonne). Bulletin du Muséum d'Histoire Naturelle de Paris 11, 201–231.
Ginsburg, L., Morales, J., Soria, D., 1994. The ruminants (Artiodactyla, Mammalia) from the Lower Miocene of Cetina de Aragón (Province of Zaragoza, Aragón, Spain). Proceedings of the Koninklijke Nederlandse Akademie van Wetenschappen 97, 141–181.
Ginsburg, L., Morales, J., Soria, D., 2001. Les Ruminantia (Artiodactyla, Mammalia) du Miocène des Bugti (Balouchistan, Pakistan). Estudios Geológicos 57, 155–170.
Goloboff, P.A., Farris, J.S., Nixon, K.C., 2008. TNT, a free program for phylogenetic analysis. Cladistics 24, 774–786.
Hassanin, A., Delsuc, F., Ropiquet, A., Hammer, C., van Vuuren, B.J., Matthee, C., Ruiz-Garcia, M., Catzeflis, F., Areskoug, V., Nguyen, T.T., Couloux, A., 2012. Pattern and timing of diversification of Cetartiodactyla (Mammalia, Laurasiatheria), as revealed by a comprehensive analysis of mitochondrial Genomes. Comptes Rendue Biologies 335, 32–50.
Huang, X.S., 1985. Fossil bovids from the middle Oligocene of Ulantatal, Nei Mongol. Vertebrata PalAsiatica 23, 152–160 (in Chinese with English summary).
Illiger, C.D., 1811. Prodromus systematis mammalium et avium additis terminis zoographicis uttriusque classis. Salfeld, Berlin, p. 301.
Janis, C.M., Manning, E., 1998. Antilocapridae. In: Janis, C.M., Scott, K.M., Jacobs, L.L. (Eds.), Evolution of Tertiary Mammals of Northern American. Volume 1: Terrestrial Canivores, Ungulates, and Ungulatelike Mammals. Cambridge University Press, Cambridge, pp. 491–510.
Janis, C.M., Scott, K.M., 1987. The interrelationships of higher ruminant families with special emphasis on the members of the Cervoidea. American Museum Novitates 2893, 1–85.
Jehenne, Y., 1985. Les Ruminants primitifs du Paleogene et du Neogene inferieur de l'Ancien Monde: Systematique, phylogenie, biostratigraphie. Ph.D. thesis. University of Poitiers, France (unpubl.).
Jehenne, Y., 1987. Intérêt biostratigraphique des ruminants primitifs du Paléogène et du Néogène inférieur d'Europe occidentale. Münchner Geowissenschaftliche Abhandlungen 10, 131–140.

Jehenne, Y., 1988. *Bedenomeryx*, un nouveau genre de Ruminant primitif de l'Oligocène supérieur et du Miocène inférieur d'Europe. Comptes Rendus de l'Académie des Sciences, Paris 307, 1991–1996.
Köhler, M., 1987. Boviden des türkischen Miozäns (Känozoikum und Braunkohlen der Türkei). Paleontologia I Evolució 21, 133–246.
Li, C.K., Qiu, Z.D., 1980. Early Miocene mammalian fossils of Xining Basin, Qinghai. Vertebrata PalAsiatica 18, 198–214 (in Chinese with English summary).
Li, J.X., Yue, L.P., Roberts, A.P., Hirt, A.M., Pan, F., Guo, L., Xu, Y., Xi, R.G., Guo, L., Qiang, X.K., Gai, C.C., Jiang, Z.X., Sun, Z.M., Liu, Q.S., 2018. Global cooling and enhanced Eocene Asian mid-latitude interior aridity. Nature Communications 9, 3026.
Linnaeus, C., 1758. Salvii, L. (Ed.), Systema naturae per regna tria naturae, secundum classes, ordines, genera, species, cum characteribus, differentiis, synonymis, locis. Tomus I. Editio decima, reformata. Holmiae [=, Stockholm, pp. 1–824.
Ma, Z.H., Peng, T.J., Li, X.M., Feng, Z.T., Guo, B.H., Li, M., Zhang, J., Song, C.H., 2021. Evolution of the main planation surfaces in the Longzhong Basin and its surrounding areas and its significance for the uplift of the Tibetan Plateau. Journal of Glaciology and Geocryology 43, 827–840 (in Chinese with English Abstract).
Made, J.V.D., 2012. *Eotragus clavatus* (Artiodactyla, Bovidae, Boselaphini) de Sansan. In: Peigné, S., Sen, S. (Eds.), Muséum National d'histoire Naturelle. Publications Scientifiques, Paris, pp. 145–199.
Marriott, K., Prothero, D., Beatty, B., 2022. Systematics of the nothokemadine camels (Artiodactyla: Camelidae). New Mexico Museum of Natural History and Science Bulletin 89, 295–302.
Marsh, O.C., 1891. A horned artiodactyle (Protoceras celer) from the Miocene. The American Journal of Science and Arts, series 3 41 (241), 81–82.
Meng, J., McKenna, M., 1998. Faunal turnovers of Palaeogene mammals from the Mongolian Plateau. Nature 394, 364–367.
Meng, J., Ye, J., Wu, W.Y., Ni, X.J., Bi, S.D., 2013. A single-point base definition of the Xiejian Age as an exemplar for refining Chinese Land Mammal Ages. In: Wang, X.M., Flynn, L., Fortelius, M. (Eds.), Fossil Mammals of Asia: Neogene Terrestrial Mammalian Biostratigraphy and Chronology of Asia. Columbia University Press, New York, pp. 124–141.
Mennecart, B., 2012. The Ruminantia (Mammalia, Cetartiodactyla) from the Oligocene to the Early Miocene of Western Europe: systematics, palaeoecology and palaeobiogeography. GeoFocus 2, 1–263.
Mennecart, B., 2015. The European ruminants during the "*Microbunodon* Event" (MP28, Latest Oligocene): impact of climate changes and faunal event on the ruminant evolution. PLoS One 10, 1–28.
Mennecart, B., Métais, G., 2015. *Mosaicomeryx* gen. nov., a ruminant mammal from the Oligocene of Europe and the significance of 'gelocids'. Journal of Systematic Palaeontology 13, 581–600.
Mennecart, B., Yerly, B., Mojon, P.O., Angelone, C., Maridet, O., Böhme, M., Pirkenseer, C., 2016. A new Late Agenian (MN2a, Early Miocene) fossil assemblage from Wallenried (Molasse Basin, Canton Fribourg, Switzerland). Paläontologische Zeitschrift 90, 101–123.
Métais, G., Antoine, P.O., Marivaux, L., Welcomme, J.L., Ducrocq, S., 2003. New artiodactyl ruminants from the late Oligocene of Pakistan. Acta Palaeontologica Polonica 48, 375–382.
Métais, G., Mennecart, B., Roohi, D.G., 2017. A new assemblage of stem pecoran ruminants from the Oligocene Chitarwata Formation, Bugti Hills, Baluchistan, Pakistan: Paleoenvironmental and paleobiogeographic implications. Journal of Asian Earth Sciences 136, 40–49.
Morales, J., Soria, D., Pickford, M., 1995. Sur les origines de la famille des Bovidae (Artiodactyla, Mammalia). Comptes Rendus de l'Académie des Sciences 321, 1211–1217.
Nishioka, Y., Hirayama, R., Kawano, S., Ogino, S.S., 2016. Lower Miocene cervoid ruminants (Artiodactyla) from the Koura Formation, Matsue, Southwestern Japan. Paleontological Research 20, 289–295.
Obergfell, F.A., 1957. Vergleichende Untersuchungen an den Dentitionen und Dentale altburdigaler Cerviden von Wintershof-West in Bayern und rezenter Cerviden (eine phylogenetische Studie). Palaeontographica Abteilung A 109, 71–166.
Owen, R., 1848. Description of Teeth and portions of Jaws of two extinct Anthracotherioid Quadrupeds (*Hyopotamus vectianus* and *Hyop. bovinus*) discovered by the Marchioness of Hastings in the Eocene Deposits on the N. W. coast of the Isle of Wight: with an attempt to develope Cuvier's idea of the Classification of Pachyderms by the Number of their Toes. Quarterly Journal of the Geological Society of London 4 (1), 103–141.
Patton, T.H., Taylor, B.E., 1973. The Protoceratinae (Mammalia, Tylopoda, Protoceratidae) and the systematics of the Protoceratidae. Bulletin of the American Museum of Natural History 150, 349–413.
Pilgrim, G.E., 1912. The vertebrate fauna from the Gaj Series in the Bugti Hills and the Punjab. Palaeontologia Indica 6, 1–83.
Prothero, D.R., 2007. Family Moschidae. In: Prothero, D.R., Foss, S.E. (Eds.), The Evolution of Artiodactyls. The Johns Hopkins University Press, Baltimore, pp. 221–226.
Prothero, D.R., 2011. Systematics of the musk deer Artiodactyla, Moschidae, Blastomerycinae from the Miocene of Nevada. Bulletin of the New Mexico Museum of Natural History and Science 53, 610–615.
Qiu, Z.D., Gu, Y.M., 1991. The Aragonian vertebrate fauna of Xiacaowan, Jiangsu: 8. *Dorcatherium* (Tragulidae, Artiodactyla). Vertebrata PalAsiatica 29, 21–37 (in Chinese with English summary).
Qiu, Z.X., Qiu, Z.D., Deng, T., Li, C.K., Zhang, Z.Q., Wang, B.Y., Wang, X.M., 2013. Neogene land mammal stages/ages of China: Toward the goal to establish an Asian land mammal stage/age Scheme. In: Wang, X.M., Flynn, L., Fortelius, M. (Eds.), Fossil Mammals of Asia: Neogene Terrestrial Mammalian Biostratigraphy and Chronology of Asia. Columbia University Press, New York, pp. 29–90.
Quiralte, V., Morales, J., 2011. *Andegameryx andegaviensis* Ginsburg, 1971 (Artiodactyla, Ruminantia,) from the early Miocene site of Estrepouy (MN3, France). Estudios Geológicos 67, 423–426.
Rincon, A.F., Bloch, J.I., Suarez, C., MacFadden, B.J., Jaramillo, C.A., 2012. New floridatragulines (Mammalia, Camelidae) from the Early Miocene Las Cascadas Formation, Panama. Journal of Vertebrate Paleontology 32, 456–475.
Rössner, G.E., 1995. Odontologische und schädelanatomische Untersuchungen an *Procervulus* (Cervidae, mammalia). Müchner Geowissenschaftliche Abhandlungen, Reihe A, Geologie und Paläontologie 29, 1–127.
Rössner, G.E., Rummel, M., 2001. *Pomelomeryx gracilis* (Pomel, 1853) (Mammalia, Artiodactyla, Moschidae) from the Lower Miocene karstic fissure filling complex Rothenstein 10/14 (Germany, Bavaria). Lynx 32, 323–353.
Sánchez, I.M., Cantalapiedra, J.L., Ríos, M., Quiralte, V., Morales, J., 2015. Systematics and evolution of the Miocene three-horned palaeomerycid ruminants (Mammalia, Cetartiodactyla). PLoS One 10, e0143034.
Scopoli, G.A., 1777. Introductio ad Historiam Naturalem, Sistens Genera Lapidium, Planatarum, et Animalium Hactenus Detecta, Caracteribus Essentialibus Donata. In: Tribus Divisa, Subinde ad Leges Naturae. :Gerle, Prague, pp. 1–540.
Sigogneau, D., 1968. Le genre *Dremotherium* (Cervoidea) anatomie du crane, denture et moulage endocranien. Annales de Paléontologie 54, 1–130.
Sokolov, I.I., 1952. Remains of Bovidae, Mammalia, from lower Miocene deposits of Western Gobi. Trudy Palaeontologičeskogo Instituta Akademii Nauk SSSR 41, 155–158 (in Russian).
Trofimov, B.A., 1958. New Bovidae from the Oligocene of Central Asia. Vertebrata PalAsiatica 2, 243–247 (in Chinese with English summary).
Viret, J., 1929. Les Faunes de Mammifères de l'Oligocène supérieur de la Limagne Bourbonnaise. Annales de l'Université de Lyon, Nouv. Sér. I Sciences, Médecine 47, 1–327.
Vislobokova, I., 1994. The Lower Miocene Artiodactyls of Tagai Bay, Olhon Island, Lake Baikal (Russia). Palaeovertebrata 23, 177–197.
Vislobokova, I., 1997. Eocene-early Miocene ruminants in Asia. Mémoires et Travaux de l'Ecole Pratique des Hautes Etudes, Inst. Montpellier 21, 215–223.
Vislobokova, I., Daxner-Höck, G., 2002. Oligocene-Early Miocene ruminants from the Valley of Lakes (Central Mongolia). Annalen des Naturhistorischen Museums in Wien 103A, 213–235.
Webb, S.D., 1998. Hornless ruminants. In: Janis, C.M., Scott, K.M., Jacobs, L.L. (Eds.), Evolution of Tertiary Mammals of Northern American. Volume 1: Terrestrial Canivores, Ungulates, and Ungulatelike Mammals. Cambridge University Press, Cambridge, pp. 463–475.
Whitworth, T., 1958. Miocene ruminants of East Africa. Fossil Mammals of Africa, British Museum (Natural History) 15, 1–50.